

This Page Is Inserted by IFW Operations
and is not a part of the Official Record

BEST AVAILABLE IMAGES

Defective images within this document are accurate representations of the original documents submitted by the applicant.

Defects in the images may include (but are not limited to):

- BLACK BORDERS
- TEXT CUT OFF AT TOP, BOTTOM OR SIDES
- FADED TEXT
- ILLEGIBLE TEXT
- SKEWED/SLANTED IMAGES
- COLORED PHOTOS
- BLACK OR VERY BLACK AND WHITE DARK PHOTOS
- GRAY SCALE DOCUMENTS

IMAGES ARE BEST AVAILABLE COPY.

**As rescanning documents *will not* correct images,
please do not report the images to the
Image Problem Mailbox.**

(19) World Intellectual Property Organization
International Bureau(43) International Publication Date
18 December 2003 (18.12.2003)

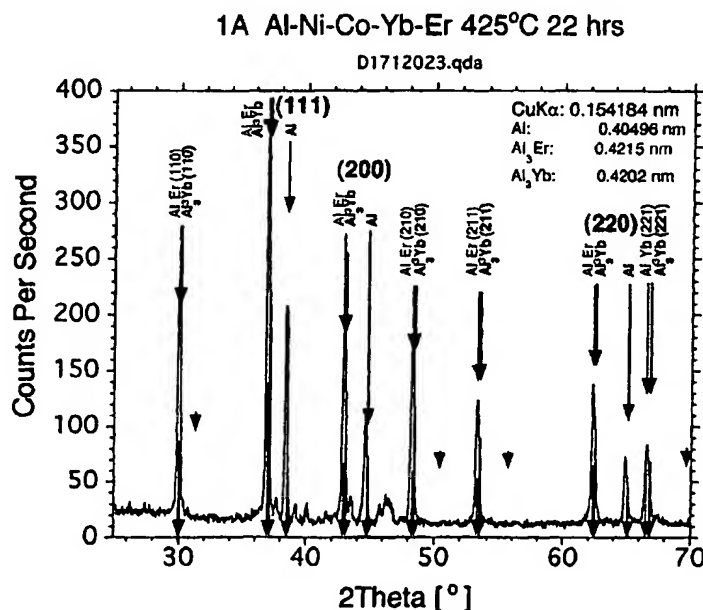
PCT

(10) International Publication Number
WO 03/104505 A2

- (51) International Patent Classification⁷: C22C
- (21) International Application Number: PCT/US03/12622
- (22) International Filing Date: 24 April 2003 (24.04.2003)
- (25) Filing Language: English
- (26) Publication Language: English
- (30) Priority Data:
60/375,940 24 April 2002 (24.04.2002) US
60/450,114 25 February 2003 (25.02.2003) US
- (71) Applicant (for all designated States except US):
QUESTEK INNOVATIONS LLC [US/US]; 1820
Ridge Avenue, Evanston, IL 60201 (US).
- (72) Inventors; and
- (75) Inventors/Applicants (for US only): OLSON, Gregory,
B. [US/US]; 1363 Kenilwood, Riverwoods, IL 60015 (US).
TANG, Weijia [CN/US]; 3144 Greenleaf Avenue, Wil-
mette, IL 60091 (US). QIU, Caian [CN/US]; 3144 Green-
leaf Avenue, Wilmette, IL 60091 (US). JOU, Herng-Jeng
[US/US]; 1210 Manor Drive, Wilmette, IL 60091 (US).
- (74) Agent: NELSON, Jon, O.; Banner & Witcoff, Ltd., 10
South Wacker Drive, Suite 3000, Chicago, IL 60606-7402
(US).
- (81) Designated States (national): AE, AG, AL, AM, AT, AU,
AZ, BA, BB, BG, BR, BY, BZ, CA, CH, CN, CO, CR, CU,
CZ, DE, DK, DM, DZ, EC, EE, ES, FI, GB, GD, GE, GH,
GM, HR, HU, ID, IL, IN, IS, JP, KE, KG, KP, KR, KZ, LC,
LK, LR, LS, LT, LU, LV, MA, MD, MG, MK, MN, MW,
MX, MZ, NI, NO, NZ, OM, PH, PL, PT, RO, RU, SC, SD,
SE, SG, SK, SL, TJ, TM, TN, TR, TT, TZ, UA, UG, US,
UZ, VC, VN, YU, ZA, ZM, ZW.
- (84) Designated States (regional): ARIPO patent (GH, GM,
KE, LS, MW, MZ, SD, SL, SZ, TZ, UG, ZM, ZW),
Eurasian patent (AM, AZ, BY, KG, KZ, MD, RU, TJ, TM),
European patent (AT, BE, BG, CH, CY, CZ, DE, DK, EE,
ES, FI, FR, GB, GR, HU, IE, IT, LU, MC, NL, PT, RO,
SE, SI, SK, TR), OAPI patent (BF, BJ, CF, CG, CI, CM,
GA, GN, GQ, GW, ML, MR, NE, SN, TD, TG).
- Published:
— without international search report and to be republished
upon receipt of that report

[Continued on next page]

(54) Title: NANOPHASE PRECIPITATION STRENGTHENED AL ALLOYS PROCESSED THROUGH THE AMORPHOUS STATE



(57) Abstract: Aluminum alloys having improved strength characteristics at elevated temperatures (300°C) are manufactured by combining selected transition metals (Ni, Co, Ti, Fe, Y, Sc) and selected rare earth materials (Er, Tm, Yb, Lu) in amounts of about 2 to 12% and 2 to 15% atomic percent respectively in an amorphous, glassy state and subsequently devitrifying the amorphous material to form a crystalline mix of fcc and L12 phase material. Devitrification from the amorphous state may be effected by various means including thermal and thermo mechanical processes.



For two-letter codes and other abbreviations, refer to the "Guidance Notes on Codes and Abbreviations" appearing at the beginning of each regular issue of the PCT Gazette.

NANOPHASE PRECIPITATION STRENGTHENED Al ALLOYS PROCESSED THROUGH THE AMORPHOUS STATE

BACKGROUND OF THE INVENTION

5 Activities relating to the development of the subject matter of this invention were funded at least in part by United States Government, U.S. Army Aviation & Missile Command Contract No. DAAH01-02-C-R125, and thus may be subject to license rights and other rights in the United States.

10 In a principal aspect, the present invention relates to aluminum-based alloys processed through an amorphous state or stage, preferably by means of a rapid solidification process from molten alloy, and then devitrified to a primarily crystalline structure by thermal or thermomechanical processing. In order to achieve a desired microstructure during processing, the aluminum alloy comprises a combination of rare earth and transition metal components with the aluminum. The final crystalline microstructure has stable high temperature strength (at
15 or above about 300°C) characterized by nanoscale intermetallic precipitates, preferably L1₂ phase precipitates.

 Currently available commercial aluminum alloys, either manufactured with ingot or powder processing, are not capable of simultaneously achieving high strength and high temperature stability near 300°C; such characteristics being particularly important in
20 applications such as the fan components in turbine engines where short-term tensile strengths of the order of 500MPa (40-60 ksi) are desired. Precipitation hardening introduced by aging is a known method to strengthen aluminum alloys. Thus, conventional high strength aluminum alloys in commercial applications utilize GP (Guinier-Preston) zones and subsequent precipitation when seeking to achieve high material strength. With this type of strengthening,
25 precipitates are usually formed during aging at or below 250°C in order to produce appropriate strengthening precipitate dispersions.

 Examples of aluminum alloys processed with relatively high aging temperatures in commercial practice include 2618 (200°C for 20 hours), 4032 (170-175°C for 8-12 hours), and 2218 (240°C for 6 hours) [Metals Handbook — Properties and Selection: Nonferrous Alloys
30 and Special-Purpose Materials, Volume 2, 10th Edition, ASM International]. At the noted aging temperatures, these alloys have improved microstructure stability relative to other commercial aluminum alloys. These aluminum alloys, when age-hardened, usually possess a room temperature yield strength of about 600Mpa (85 ksi). However, at temperatures approaching

300°C, the precipitation strengthening efficiency in these alloys quickly and significantly degrades as a result of precipitate coarsening and/or dissolution. Due to the unstable strengthening precipitate size distribution at such high temperatures, the yield strength of currently available aluminum alloys at 300°C is often only 10% of the yield strength at room temperature, and thus renders such alloys unsuitable for high temperature applications above 150°C.

In order to achieve a combination of high strength and usable high temperature properties in aluminum alloys, researchers have investigated a variety of intermetallic precipitation dispersions. Since selected intermetallic precipitates may determine the strength and ductility of the final aluminum alloy, it is desirable to select cubic precipitate phases with high crystallographic symmetry to promote ductility. The aluminum-based $L1_2$ phase (fcc ordered) is one of the best-known precipitates to achieve a good combination of high strength and high toughness.

However, since crystalline aluminum has very limited solubility for most intermetallics, including $L1_2$ forming components, it is difficult to produce fine intermetallic dispersions through crystalline solid-state heat treatments that utilize a step to dissolve the strengthening phase particles prior to reprecipitation during aging. However, rapid solidification processing (RSP) from the liquid state has been attempted or utilized. With an RSP process, it is possible to either (1) directly produce fine crystalline structure, or (2) produce partially or completely amorphous aluminum alloys. Nonetheless, crystalline RSP aluminum alloys have not been able to meet the high temperature strength requirements due to the difficulty of producing small, stable particle sizes at adequate volume fraction. Alternatively, the focus on amorphous aluminum alloys has been primarily on the glass formability. These glassy alloys in general have low ductility, and, when devitrified, they typically form crystalline microstructures that are far from optimal for fracture toughness and other requirements.

For example, RSP crystalline aluminum alloys, not designed to form glass with RSP, utilize a metastable and coherent $L1_2$ dispersion (about 1%) which converts into other phase structures at high temperature. [Parameswaran, Weertman and Fine, Scripta Metall., vol.23, pp.147, 1989] U.S. Pat. Nos. 4,950,452, 5,074,935, 5,334,266, 5,458,700, 5,431,751, 5,053,085 and its derived divisional patents (U.S. Pat. Nos. 5,240,517, 5,320,688, and 5,368,658) utilize RSP to achieve either amorphous, a mixture of amorphous and crystalline, or crystalline microstructures, without the use of an $L1_2$ strengthening dispersion. The aluminum alloys of U.S. Pat. No. 4,889,582 achieve the high temperature strength with RSP process and age

hardening to produce Al_3Fe (which has non-cubic DO_3 , not L_{12} structure) strengthening precipitates, using different alloying components. U.S. Pat. No. 4,464,199 describes high strength aluminum alloys with 4 to 15% iron processed with RSP to achieve high temperature stability. Use of iron promotes Al_3Fe precipitation.

5 The aluminum alloys of U.S. Pat. No. 4,787,943 are composed of transition metals and rare earth metal components. However, with titanium and iron as the preferred transition metals, and gadolinium and cerium as rare earth elements, the alloy does not comprise a stable L_{12} strengthening dispersion.

10 U.S. Pat. No. 6,248,453B1 describes the use of an L_{12} strengthening dispersion for high strength aluminum alloys utilizing certain alloying components, but does not utilize a transition metal such as nickel and cobalt and an intermediate amorphous state as a means to refine the L_{12} microstructure.

15 Finally, the high strength and high temperature aluminum alloys referenced have not found widespread application due to the lack of robust processing to produce those alloys and the deficiency of other alloy properties, such as toughness and ductility.

SUMMARY OF THE INVENTION

20 The present invention is directed to a new class of aluminum alloys characterized by formation from an intermediate amorphous state to a final face centered cubic (fcc) aluminum matrix strengthened by a precipitate dispersion in order to achieve high temperature strength with usable ductility. The disclosed aluminum alloys thus are comprised of a fine crystalline structure of primarily aluminum fcc matrix strengthened by a precipitate phase with high cubic symmetry, preferably the L_{12} phase. An appropriate melt of aluminum with crystalline formers is first processed to achieve an intermediate amorphous state to preserve the crystalline
25 formers. The preferred method to achieve a primarily (above 70% in volume) amorphous state is a rapid solidification process (RSP) from the molten alloy by process techniques such as powder atomization, melt spinning, and spray casting. The RSP process preferably should have a cooling rate of at least about 10^3 °C/sec, preferably at least 10^4 °C/sec. Other methods to achieve amorphous microstructure through a solid-state process, such as mechanical milling,
30 may also be used. The intermediate amorphous alloys are then devitrified to a final primarily (above 70% in volume) fcc/ L_{12} crystalline microstructure with at least about 30% fcc phase in volume and at least about 10% L_{12} phase in volume. Thermal treatment, thermomechanical

treatment, or a combination of both, are the preferred methods to produce the final crystalline microstructure.

The alloys of the invention demonstrate high strength capability after both short and long exposure to a high temperature at or above 300°C by maintaining a fine and stable microstructure. For example, a short-term strength requirement of 40 – 60 ksi yield strength is expected. For the long-term strength, as characterized by creep strength, it has been demonstrated that optimal creep resistance at 300°C for aluminum alloys is obtained from a dispersion of 25 nm diameter L1₂ particles [E. A. Marquis, *Microstructural Evolution and Strengthening Mechanisms in Al-Sc and Al-Mg-Sc Alloys*, Ph.D. thesis, Northwestern University, 2002.]. Also, it has been demonstrated [Ohtera, Inoue and Masumoto, in *First International Conference on Processing Materials for Properties*, Ed. Henein and Oki, The Minerals, Metals & Materials Society, p.713, 1993] that aluminum-based alloys devitrified by extrusion from amorphous atomized powder can achieve aluminum fcc grain size of 80 to 170 nm, with intermetallic phase dispersions as fine as 10 to 80 nm in diameter. Such grain or particle sizes may therefore encompass the desired optimal particle diameter for creep strengthening by an L1₂ phase intermetallic dispersion. Accordingly, a process and an aluminum alloy product combining a sufficient amount of stable L1₂ refined or converted by devitrification from a glass phase material by appropriate thermal or thermomechanical processing has been discovered. The alloy meets or exceeds high temperature strength requirements with optimized creep resistance as a result of intermetallic, small particle phase dispersions.

The aluminum alloys of this invention are produced by combining aluminum, selected metals, particularly transition metals, rare earth elements, and other optional elements into a melt which is converted to an amorphous or glassy state and then subsequently to a crystalline state by a devitrification process. In the broadest sense about 2 to 15 atomic percent in the aggregate of at least one rare earth selected from the group consisting of erbium (Er), thulium (Tm), ytterbium (Yb) and lutetium (Lu) is provided for the melt. Further about 2 to 7 atomic percent in the aggregate of at least one transition metal selected from the group consisting of nickel (Ni), cobalt (Co), iron (Fe) and copper (Cu) is provided to enhance or facilitate the process step of forming an amorphous or glassy material from the melt. Other materials included, optionally, in the melt comprise additional transition metals, lithium (Li) and magnesium (Mg). For example, of less than about 5% in the aggregate by atomic fraction scandium (Sc), yttrium (Y), titanium (Ti), zirconium (Zr), vanadium (V), chromium (Cr),

manganese (Mn) and lithium (Li) incorporated into the melt or alloy as a modifier. Less than about 7% in the aggregate by atomic fraction magnesium (Mg), zinc (Zn), silver (Ag) and niobium (Nb) may be incorporated into the melt or alloy to accommodate fcc misfit in the crystalline state.

5 The selection of alloying components is based on the function or criteria of (1) good L₁₂ formers, (2) adequate glass formability with RSP — this leads to the selection of components with strong short range ordering effects and slow long-range diffusing kinetics in molten aluminum, and (3) good fcc/L₁₂ coherency with low misfit which lead to a fine microstructure and good coarsening resistance at high temperature.

10 Lanthanide rare earth L₁₂ formers such as erbium (Er), thulium (Tm), ytterbium (Yb), and lutetium (Lu) are slow diffusers and hence enhance glass formability while at the same time allowing L₁₂ formation during devitrification. Scandium (Sc) is a strong L₁₂ former which can be used in conjunction with rare earth components to promote L₁₂ formation and reduce the misfit between fcc and L₁₂ phases. Transition metals such as nickel (Ni), cobalt (Co), iron
15 (Fe), and copper (Cu) can enhance short range ordering in the molten aluminum, leading to the increase of glass transition temperature and promoting glass formability. Magnesium (Mg), as a component with relatively high solubility in crystalline aluminum, can be used in fcc aluminum to further reduce the fcc/L₁₂ misfit.

20 With efficient precipitation strengthening by the L₁₂ dispersion, the alloys of the subject invention achieve a hardness of 490 VHN at significantly higher aging temperature compared to conventional aluminum alloys indicating a usable strength at or beyond 300°C.

25 Thus, it is an object of the invention to provide a new class of high-strength L₁₂ phase strengthened aluminum alloys processed into the amorphous state, preferably with a rapid solidification process, and then subsequently devitrified into a crystalline structure with a thermomechanical or thermal processes.

30 A further object of the invention is to provide aluminum alloys with usable strength at or above 300°C by selecting (1) slow diffusing L₁₂ formers to prevent fast coarsening kinetics at high temperature, (2) appropriate matrix fcc and L₁₂ components to reduce the lattice misfit between them to further slow down the coarsening kinetics and to promote the initial finer L₁₂ morphology.

 Another object of the invention is to utilize the cubic crystal structure of L₁₂ phase to promote the interfacial coherency with an aluminum fcc matrix and the inherent ductile

behavior of the $L1_2$ crystalline phase itself, due to high number of slip systems in cubic $L1_2$ structure, to maintain reasonable overall alloy ductility.

A further object of the invention is to combine alloying components so that the $L1_2$ formation is enhanced while the likelihood of forming other undesirable intermetallics is reduced, in order to further promote alloy ductility of an aluminum alloy.

Another object of the invention is to provide adequate glass formability during the rapid solidification process such as powder atomization or melt spinning to form an amorphous aluminum alloy structure, preserving the $L1_2$ formers in the solution before a subsequent devitrification process.

A further object of the invention is to utilize the intermediate, highly supersaturated amorphous state, slow $L1_2$ coarsening kinetics, and low $L1_2$ /fcc misfit to produce a fine microstructure in a strong aluminum alloy.

A further object of the invention is to provide aluminum alloys having high strength at high temperatures with appropriate toughness when processed with powder metallurgy techniques through an amorphous state.

Another object of the invention is to combine transition metals and rare earth components to provide sufficient glass formability during a rapid solidification process and a nanoscale $L1_2$ dispersion strengthened aluminum alloy fcc crystalline structure after devitrification.

These and other objects, advantages and features will be set forth in the detailed description which follows.

BRIEF DESCRIPTION OF THE DRAWING

In the detailed description which follows, reference will be made to the drawing comprised of the following figures:

Figure 1 is a chart setting forth criteria for the design of aluminum alloys of the invention;

Figure 2 is a diagram illustrating the viscosity of liquid aluminum nickel alloys calculated at 1700°C in comparison with experimental data wherein the comparison is based upon calculations made using different thermodynamic descriptions of the aluminum nickel liquid (substitutional solution model without associate or associate model with AlNi associate);

Figure 3 is an assessed Al – Yb phase diagram in comparison with experimental data;

Figure 4a is a graph of the enthalpy of formation of cobalt and a rare earth, i.e. Er and Yb predicted by quantum mechanical calculation;

Figure 4b is a graph of the mixing enthalpy of the materials set forth in Figure 4a;

Figure 4c is a graph of the molar volume of the materials set forth in Figure 4a;

5 Figure 5 is an X-ray diffractogram of the alloy of Example 1A as melt-spun with positions of fcc pure aluminum reflections indicating a fully amorphous state;

Figure 6 is an isochronic DSC thermogram of the alloy of Example 1A indicating devitrification steps upon heating;

10 Figure 7 is an X-ray diffractogram of the alloy of Example 1A after devitrification at 425°C for 22 hours, with positions of reflections of pure fcc Al, Al_3Yb , and Al_3Er phases, indicating the desired phases: FCC+ L_{12} ;

Figure 8 is a SIMS elemental map of devitrified alloy of Example 1A indicating Er and Yb partition together to L_{12} phase, and Ni and Co which do not partition to L_{12} ;

15 Figure 9 is a scanning electron microscope (SEM) secondary electron image of devitrified alloy of Example 1A indicating submicron morphology;

Figure 10 is a 3DAP microscopy reconstruction of $\text{Al}_3(\text{Yb,Er})\text{L}_{12}$ phase of the alloy of Example 1A after devitrification at 424°C for 19 hours;

Figure 11 is an X-ray diffractogram of the alloy of Example 2A as melt-spun, with positions of fcc pure Al and L_{12} reflections, indicating fully amorphous status;

20 Figure 12 is an X-ray diffractogram of the alloy of Example 2A after devitrification at 425°C for 19 hours, with positions of reflections of pure fcc Al, Al_3Yb , and Al_3Er phases, indicating the desired phases: FCC+ L_{12} ;

Figure 13 is an X-ray diffractogram of the alloy of Example 2B as melt-spun, with positions of fcc pure Al and L_{12} reflections, indicating fully amorphous status;

25 Figure 14 is an X-ray diffractogram of the alloy of Example 2B after devitrification at 425°C for 19 hours, with positions of reflections of pure fcc Al, Al_3Yb , and Al_3Er phases, indicating the desired phases: FCC+ L_{12} wherein the lattice parameter of L_{12} is reduced by Sc;

Figure 15 is an X-ray diffractogram of the alloy of Example 2C as melt-spun, with positions of fcc pure Al and L_{12} reflections, indicating almost fully amorphous status;

30 Figure 16 is an X-ray diffractogram of the alloy of Example 2C after devitrification at 425°C for 19 hours, with positions of reflections of pure fcc Al, Al_3Yb , and Al_3Er phases, indicating the desired phases: FCC+ L_{12} wherein the lattice parameter of L_{12} is expanded by Mg;

Figure 17 is an X-ray diffractogram of the alloy of Example 2D as melt-spun, with positions of fcc pure Al and $L1_2$ reflections, indicating fully amorphous status;

Figure 18 is an X-ray diffractogram of the alloy of Example 2D after devitrification at 425°C for 19 hours, with positions of reflections of pure fcc Al, Al_3Yb , and Al_3Er phases, indicating the desired phases: FCC+ $L1_2$ and wherein the lattice parameter of fcc is expanded by Mg and that of $L1_2$ is reduced by Sc;

Figure 19 is an X-ray diffractogram of the alloy of Example 1C as melt-spun, with positions of fcc pure Al and $L1_2$ reflections, indicating non-amorphous status due to the absence of transition metal elements;

Figure 20 is an X-ray diffractogram of the alloy of Example 1C after devitrification at 425°C for 19 hours, with positions of reflections of pure fcc Al, Al_3Yb , and Al_3Er phases, indicating elements ER, Yb, and Sc can be completely intersoluble to form $L1_2$ and wherein the lattice parameter of $L1_2$ is reduced by Sc; and

Figure 21 is a scanning electron microscope (SEM) secondary electron image of a devitrified alloy of Example 1C showing coarse microstructure in comparison with the alloy of Example 1A (see Figure 9) and indicating that passing through the glassy state can reduce the particle size of precipitation.

DESCRIPTION OF THE PREFERRED EMBODIMENTS

General Summary

In general, the subject matter of the invention comprises a product (alloy) as well as a product by process and a process all directed to an aluminum alloy in crystalline form having higher or greater strength particularly at elevated temperatures, i.e. greater than at least 250°C and preferably 300°C. The alloy of aluminum is made by compounding a mixture of aluminum with selected rare earths (RE) and transition metals (TM) in an amorphous or glassy state followed by devitrification of the material from the amorphous state to a mixed crystalline state comprised of face centered cubic (fcc) and $L1_2$. (an ordered fcc) state wherein the ratios of the crystalline states is within certain preferred ranges. Preferably the resultant alloy has at least about 30% by volume fcc phase and at least about 10% by volume $L1_2$ phase material with limited residual amorphous or other phase material such as quasi-crystalline or ordered amorphous material.

The choice of starting materials may be varied as may the compounding processes, the glass phase formation processes and the devitrification processes. Importantly, when in the amorphous state, there may be some crystalline material contained therein, but preferably no more than about 30% by volume in the fcc phase. Thus forming the mixture in the amorphous or glassy intermediate state and subsequent devitrification constitute very important aspects of the invention.

The alloy materials, in addition to aluminum (Al), include one or more lanthanide rare earths (RE) selected or taken from the group of erbium (Er), thulium (Tm), ytterbium (Yb), and lutetium (Lu), and one or more transition metals (TM) taken or selected from the group of copper (Cu), nickel (Ni), cobalt (Co), titanium (Ti), iron (Fe), yttrium (Y), and scandium (Sc). Further additives in minor amounts (less than about five percent (5%) atomic percent) may be included such as magnesium (Mg). The range of various constituents is also important to maintain processability and preserve transition characteristics. Thus RE materials are utilized in the range of about 2 to 15 atomic percent (%), and the TM and metals are utilized in the aggregate range of about 2 to 12 atomic percent (%). Transition metals (TM) in the range of about 2 to 7 atomic percent are utilized.

The processes for mixing or forming the starting materials in the amorphous state are not necessarily limiting. Thus, it is contemplated that solid state processing, liquid or melt processing as well as gas phase processing may be utilized, though liquid phase processing is preferred based upon examples as reported hereinafter. The completeness of the amorphous state is preferably at least about 70% by volume and preferably greater. The amorphous state is a solid noncrystalline state or phase prior to devitrification.

Development Technique

Devitrification is accomplished via heat treating (thermal) processing, thermo-mechanical processing as well as other processing techniques.

Precipitation strengthened aluminum (Al) alloys are difficult to develop for high strength due to limited solubility of alloying elements in fcc Al. The low solubility of strengthening dispersion elements prevents the solid-state solution treatment of the alloy to bring strengthening components into solution. It is hence not necessarily possible to allow subsequent aging to produce a desirable strengthening microstructure. Al alloys with high fractions of precipitate that cannot be completely solution treated therefore have very coarse particle sizes that tend to limit strength, corrosion resistance and toughness. In contrast, the Al alloys exhibit composition

and microstructure characteristics that enable the Al alloys of invention to exhibit high strength, good ductility, and high temperature stability at or above 300°C.

By selecting an appropriate composition, processing techniques achieve a fully amorphous state after rapid cooling of the Al alloy composition. Furthermore, with careful selection of composition this glass can then be thermal or thermo-mechanically processed such that the glass devitrifies into a fully crystalline fcc matrix with intermetallic precipitates having a very fine size scale. By passing through the glass state, the equilibrium solidification that would produce coarse precipitates is avoided. Furthermore, the selection of the precipitate phase as L1₂ allows the precipitate to be coherent or semi-coherent with the fcc matrix improving the ductility of the alloy and the resistance of the precipitate to coarsen during subsequent thermal treatment.

Figure 1 is a system flow-block diagram that illustrates the processing/structure/properties relationships for alloys of the invention. The two-stage nature of the chart emphasizes the generally equal importance of processability and final performance in the design of alloys of the invention. The processability is governed by the glass forming ability; strength, ductility, and thermal stability are the required end properties.

Certain transition metals (TM) (such as Fe, Co, Ni, Cu) promote short-range ordering in liquid Al, which leads to low partial molar volume, low thermal expansion, and high viscosity that are beneficial to glass forming ability. Rare-earth (RE) elements (such as Ce, Gd, Yb, Er) with large atomic size exhibit low diffusivity in Al and thus retard crystal nucleation. Therefore, Al-TM-RE comprise a class of glass forming system for Al alloys.

Viscosity of liquid metals also has a strong effect on the glass forming ability. Liquid phase metals having high viscosity usually becomes glass through fast cooling. A binary model to describe liquid's viscosity is set forth in Equation (1):

$$\eta = -\frac{x_1 x_2}{RT} (x_1 \eta_1^o + x_2 \eta_2^o) \frac{\partial^2 G_m}{\partial x_2^2} \quad (1)$$

The variables x_i and G_m represent the mole fraction and molar Gibbs energy of the liquid, respectively. The viscosity of pure components, η_i^o , is available from literature, see Table 1. From the above equation it is seen that the composition dependence of the viscosity is fully determined by the thermodynamic properties of the liquid.

Table 1. Viscosity and related data for pure liquid metals
 [L. Battezzati and A.L. Greer, "The Viscosity of Liquid Metals and Alloys," *Acta metall.* 37, 1791 (1989).]

Element	T_m (K)	V_m (10^{-6} m^3/mol)	$\eta(T_m)$ (10^{-3} Pa s)	C_A [10^{-7} (J/K mol ^{1/3}) ^{1/2}]	E (kJ/mol)	B (E/RT _m)	η_0 (10^{-3} Pa s)
Al	933	11.3	1.30	1.30	16.5	2.13	0.149
Co	1765	7.59	4.18	1.58	44.4	3.03	0.255
Cr	2133	8.28	5.7	~2.2	~185	~10.43	1.7×10^{-4}
Cu	1356	7.94	4.0	1.72	30.5	2.71	0.301
Fe	1809	7.96	5.5	2.18	41.4	2.75	0.370
Mn	1517	9.58	5	2.5	20-46.5	1.6-3.7	0.12-1.02
Ni	1728	7.43	4.90	1.85	50.2	3.49	0.166
V	2175	8.9	2.4	0.98	~73	~4.04	~0.042
Ti	1958	11.6	2.2	1.18	~68	~4.18	~0.034
Zr	2125	~15.7	3.5	1.58	~88	~4.98	~0.024

T_m : melting temperature

V_m : molar volume at T_m

$\eta(T_m)$: viscosity at T_m

C_A : constant

E: activation energy for viscous flow

B: $B = E/RT_m$

η_0 : pre-exponential viscosity

Equation (1) has been validated for several binary systems where both experimental viscosity data and thermodynamic descriptions are available. An example is the Al-Ni system where an intermediate compound AlNi melts congruently at about 1650°C. Figure 2 shows the calculated viscosity in Al-Ni liquid at 1700°C as a function of Ni content, in comparison with experimental data. It is seen that the calculated viscosity shows a similar trend as the experimental data, but the latter indicates a stronger increase of the viscosity around 50 at.% Ni. The strong increase in viscosity is believed to be caused by molecular associates of Al-Ni in the liquid. In order to illustrate the effect of the AlNi associates on the viscosity, the Al-Ni system was thermodynamically reassessed with an associate model for the liquid free energy. The viscosity of Al-Ni liquid calculated using the AlNi associate model is also plotted in Figure 2 for comparison. The calculation shows a significant increase in the viscosity due to the formation of liquid AlNi associates.

This viscosity model has further been extended to multi-component systems, which provides guidance of glass forming ability for the design of alloys of the invention.

A model to predict glass transition temperature, T_g , has been developed for the Al-TM-RE system. The model is based on the parabolic relationship between T_g and room temperature glass shear modulus, G, and it assumes that G is linear in atomic fraction, X, of each element according to equation (2):

$$T_g = \left(14100 \sum_i K_i X_i \right)^{0.49} \quad (2)$$

$i = Al, Mg, Ni, Co, Er, Yb, Sc, Y, etc.$

The coefficient for each element, K_i , has been calibrated to experimental DSC data of melt-spun amorphous ribbons. These coefficients quantitatively represent the relative effectiveness of the aforementioned molecular associates in promoting glass forming ability by varying T_g . This model also provides guidance of glass forming ability for the design of alloys of the invention. The prediction error of equation (2) compared to available experimental data is about 9 K with a standard deviation of 10 K, which is within the experimental precision.

The desired performance for applications (e.g. aircraft structural components, high temperature turbine components, etc.) determines a set of alloy properties required, including strength, ductility and thermal stability resistance up to 300°C. The desired properties can be achieved through a fine, stable, multicomponent $L1_2$ phase dispersion in the Al matrix after devitrification of the glassy Al, as long as a sufficient volume fraction of $L1_2$ and low misfit with the Al matrix and thus low coarsening rate can be obtained.

The elements Er, Lu, Tm and Yb are known as the only stable rare earth (RE) $L1_2$ formers. The melting point and cost of these rare earth elements are presented in Table 2. Some properties of corresponding trialuminides are also given in Table 2, including lattice parameter, density, and $L1_2$ decomposition or congruent melting temperature. Among the four RE elements, according to Table 2, Yb has the smallest lattice parameter and relatively lower cost. Er has the lowest cost. Both Yb and Er have relatively lower melting point. Usually, the lower the melting temperature, the higher the glass forming ability. As a consequence, Alloys of the invention utilize Yb and Er as preferred $L1_2$ formers rather than Tm and Lu.

Table 2. Stable $L1_2$ formers and their properties.

Element	Melting Point	Cost ^a	$L1_2$	Lattice Parameter	Density	$L1_2$ Max. Temp.
Er	1529°C	\$725/kg	Al_3Er	4.226 Å	5.507 g/cm ³	1070°C
Lu	1663°C	\$7500/kg	Al_3Lu	4.186 Å	5.783 g/cm ³	1200°C
Tm	1545°C	\$6500/kg	Al_3Tm	4.203 Å	5.591 g/cm ³	
Yb	819°C	\$1600/kg	Al_3Yb	4.202 Å	5.682 g/cm ³	980°C
Sc	1541°C	\$18,000/kg	Al_3Sc	4.101 Å	3.03 g/cm ³	1320°C

^a For 1-5 kg cast metal ingots from 99.9%-grade oxides

Sc is the only transition metal (TM) element that can form a stable $L1_2$ with Al. In comparison with RE $L1_2$ formers, Sc can form $L1_2$ with a smaller lattice parameter of 4.101 Å,

thus leading to smaller misfit between L1₂ and the Al matrix. However, Sc is by far the most expensive of the elements considered, as seen in Table 2. The alloy of the invention therefore seeks to limit the use of Sc as much as possible. Efforts have been made to search for other transition metals to substitute for Sc. A preliminary requirement for such substitution is solubility. Experiments have shown that Ti has a substantial solubility in Al₃Sc, up to 12.5 at.%, i.e. Al_{0.75}Sc_{0.125}Ti_{0.125}. In addition, Ti has the lowest diffusion coefficient in solid Al among the transition metals. For instance, the diffusivity in Al at 300°C is 9.0×10⁻²⁰ m²/s for Sc, 6.3×10⁻²⁴ m²/s for Zr, and 2.7×10⁻²⁵ m²/s for Ti. Adding Ti to Al₃Sc will thus reduce the coarsening rate of L1₂ precipitates. Moreover, addition of Ti decreases the lattice parameter of Al₃(Sc,Ti) and hence minimizes the lattice misfit with Al. The lattice parameters for seven hypothetical L1₂ compounds with transition metals are calculated at zero degree Kelvin (0 K) using the first-principle quantum mechanical approach. Results are shown in Table 3. All seven hypothetical L1₂ compounds show significant smaller lattice parameters than those stable L1₂ phases. Thus, alloys of the invention incorporate Yb, Er and Sc as base L1₂ formers but are not limited to these elements. TMs such as Ti, V, Zr, etc, which will result in low misfit and thus lower interfacial energy to yield a low driving force for particle coarsening are considered useful.

Table 3 Lattice Parameters of hypothetical L1₂ TM Compounds through First Principle Calculations at 0 K.

TMs Hypothetic L1 ₂	Lattice Parameter, Å
Al ₃ Ti	3.967
Al ₃ Zr	4.085
Al ₃ V	4.045
Al ₃ Fe	3.8005
Al ₃ Ni	3.8469
Al ₃ Co	3.7946
Al ₃ Cu	3.9363

It should be pointed out that the compound Al₃Ti is metastable as the L1₂ phase but stable as D0₂₂. It can be transformed to the L1₂ structure if Al is substituted partially by Cr, Mn, Fe, Co or Ni.

For a multicomponent L1₂ phase, the lattice parameter a can be calculated based on a linear model similar to Vegard's law. As an example, we have the following equation for L1₂ with the formula Al₃(Er_xYb_ySc_z) is utilized:

$$a[\text{Al}_3(\text{Er}_x\text{Yb}_y\text{Sc}_z)] = x * a(\text{Al}_3\text{Er}) + y * a(\text{Al}_3\text{Yb}) + z * a(\text{Al}_3\text{Sc}) \quad (3)$$

Assuming $L1_2$ has a linear thermal expansion, its lattice parameter at elevated temperature can be calculated as follows (T in $^{\circ}\text{C}$):

$$a(L1_2, T) = a(L1_2, RT) \times [1 + (T - 25) \times \alpha(L1_2)] \quad (4)$$

where $\alpha(L1_2)$ represents the thermal expansion estimated according to the following reciprocal relation:

$$\frac{\alpha(M)}{\alpha(Al_3M)} = \frac{T_m(Al_3M)}{T_m(M)} \quad (5)$$

where M represents the corresponding pure metal in Al_3M and T_m is the melting point ($^{\circ}\text{K}$).

Table 4 summarizes melting point, thermal expansion of relevant elements in alloys of the invention and the estimated thermal expansion as well as lattice parameter at 25°C and 300°C

for stable $L1_2$ or meta-stable $L1_2$.

Table 4. Estimation of Thermal Expansion Coefficients and Lattice Parameters.

Element	Melting Point, $^{\circ}\text{K}$	Thermal Expansion, $1/^{\circ}\text{K}$, $20\sim 100^{\circ}\text{C}$	Thermal Expansion, $1/^{\circ}\text{K}$, $20\sim 300^{\circ}\text{C}$	$L1_2$ Alloys	Melting Point, $^{\circ}\text{K}$	Thermal Expansion, $20\sim 300^{\circ}\text{C}$	Lattice Parameter, \AA , 25°C	Lattice Parameter, \AA , 300°C
Ni	1728	13.3×10^{-6}	14.4×10^{-6}	Al_3Ni	913	27.254×10^{-6}	3.8639	3.8929
Co	1768	12.5×10^{-6}	13.6×10^{-6}	Al_3Co	1408	17.077×10^{-6}	3.8114	3.8293
Yb	1092	25×10^{-6}	25×10^{-6}	Al_3Yb	1253	21.788×10^{-6}	4.202	4.2272
Er	1802	9.2×10^{-6}	9.2×10^{-6}	Al_3Er	1343	12.344×10^{-6}	4.226	4.2403
Sc	1814	12×10^{-6}	12×10^{-6}	Al_3Sc	1593	13.665	4.101	4.1164
Ti	1943	8.9×10^{-6}	9.2×10^{-6}	Al_3Ti	1623	11.014	3.967	3.979
Y	1795	10.8×10^{-6}	10.8×10^{-6}	Al_3Y	1253	15.472	4.299	4.3173
Al			25.3×10^{-6}				4.0497	4.0779

In the practice of the invention, decrease of the misfit by expanding the lattice parameter of the Al matrix is a useful technique. There are few elements that have significant solubility in Al. Mg is the only one that can substantially increase the lattice spacing of Al. According to literature information, in dilute AlMg alloys, every one atom percent of Mg will expand the Al lattice by 0.0045 \AA . Further, every one atom percent of Mg will increase the linear coefficient of thermal expansion of Al by $1.179 \times 10^{-7}/^{\circ}\text{C}$.

Thermodynamic modeling and assessments have been performed for Al-TM-RE systems with relevant elements incorporated in alloys of the invention. The assessed Al-Yb binary phase diagram is shown in Figure 3. The $L1_2$ Al_3Yb is the strengthening phase that is used in alloys of the invention. According to Figure 3, Al_3Yb is not solution treatable. The only way to avoid coarse precipitation from Al liquid is using fast cooling. It is possible to get fine

crystalline precipitates directly by rapid solidification processing (RSP) from the melt. However, much finer precipitates can be generated through devitrification of amorphous state due to the larger driving force. In addition, the precipitation process can be controlled through devitrification.

5 Quantum mechanical calculations have been performed in $\text{Al}_3\text{Er-Al}_3\text{Co}$ and $\text{Al}_3\text{Yb-Al}_3\text{Co}$ systems. The predicted enthalpy of formation, mixing enthalpy and molar volume in the corresponding systems are plotted in Figure 4. According to Figure 4, there is a strong repulsive Co-RE interaction indicating negligible Co solubility in L_{12} Al_3RE . This sets a challenge in producing good glass forming alloys through conventional technology in the same composition intended to precipitate a significant amount of L_{12} precipitation through devitrification.

Experimental Results

15 The present invention alloys, through computational design of multi-component Al-TM-RE systems incorporate, desired processing properties – glass forming ability and the desired microstructure – a fine dispersion of L_{12} after devitrification in the Al matrix. Alloys of the invention are summarized in Table 5 for their composition, status in melt-spun and devitrification conditions, as well as the lattice parameter of the Al fcc and the L_{12} phases and the misfit between L_{12} and Al matrix.

Table 5 Summary of Composition and Microstructure of Al Alloys

No.	Alloy Composition at. %	As-spun status	Main phases after devitrification	Lattice Parameter		Misfit %
				L1 ₂ , a(Å)	fcc, a(Å)	
1A	Al-2.5Ni-2.5Co -3.5Yb-3.5Er	fully glass	fcc, L1 ₂ + minor x phase	4.215	4.063	3.735
1B	Al-2.75Ni-2.75Co-2.17Yb -2.17Er-2.17Y	fully glass	fcc, L1 ₂ +Al ₃ Y+ minor x phase	4.217	4.050	4.123
1C	Al-6Yb-6Er	fcc, L1 ₂ + some glass	fcc, L1 ₂	4.208	4.057	3.726
1D	Al-4Yb-4Er-4Y	fcc, L1 ₂ + some glass	fcc, L1 ₂ + Al ₃ Y	4.229	4.059	4.192
1E	Al-4.5Yb-4.5Er-3Sc	fcc, L1 ₂ + some glass	fcc, L1 ₂	4.183	4.060	3.032
1F	Al-12Er-3Mg	fcc, L1 ₂ + some glass	fcc, L1 ₂	4.216	4.059	3.865
1G	Al-12Er-6Mg	fcc, L1 ₂ + some glass	fcc, L1 ₂	4.217	4.065	3.739
1H	Al-12Yb-3Mg	fcc + some glass	fcc, L1 ₂	4.216	4.076	3.435
1I	Al-12Yb-6Mg	fcc, L1 ₂ + some glass	fcc, L1 ₂	4.191	4.061	3.201
2A	Al-2Ni-2Co-4Yb-4Er	almost fully glass+minor fcc	fcc, L1 ₂ + minor x phase	4.201	4.049	3.754
2B	Al-2.5Ni-2.5Co-2Yb- 2Er-3Sc	almost fully glass+minor fcc	fcc, L1 ₂ + minor x phase	4.150	4.048	2.520
2C	Al-3Mg-2.5Ni-2.5Co- 4.5Yb-2.5Er	mostly glass + minor fcc	fcc, L1 ₂ + minor x phase	4.197	4.060	3.374
2D	Al-3Mg-2.5Ni-2.5Co- 2.5Yb-1.5Er-3Sc	fully glass	fcc, L1 ₂ + minor x phase	4.155	4.057	2.416

According to Table 5, alloys with TM elements (e.g. Ni and Co) are fully glass or almost fully glass in the as melt-spun conditions. These alloys include alloy 1A, 1B, 2A, 2B, 2C and 2D. Alloys without Ni and Co primarily show FCC Al and L1₂ crystalline phases although they are partially amorphous in the as melt-spun conditions. These alloys include alloy 1C, 1D, 1E, 1F, 1G, 1H and 1I. The results confirm the prediction that TM elements such as Ni and Co are critical elements to promote the glass forming ability in the alloys of the invention. Through devitrification, all alloys precipitate mainly L1₂ in the Al matrix. It should be emphasized that the particle size of alloys passing through a fully or almost fully glassy state is much finer than that of alloys without passing through the glassy state or only passing through a partially glassy state with L1₂ already present in the as-spun condition.

Following is a detailed demonstration of characteristics of alloys in Table 5.

Example 1

Alloy 1A in Table 5 was fabricated into both powders using gas atomization and ribbons using melt spinning technology (wheel speed 55 m/s). In the as melt-spun condition, Alloy 1A was initially characterized by X-ray diffraction (XRD) and differential scanning calorimetry (DSC). The diffractometer trace (Cu-K α radiation) of as-spun Alloy 1A in Figure 5 shows a broad peak characteristic of glass, and the ribbons show very good ductility, also characteristic of the glassy state. A DSC trace run at 40°C/min. shown in Figure 6 indicates three stages of glass devitrification at temperatures near 200°C, 315°C and 370°C.

DSC thermograms indicated that for heating at a constant rate of 10-40°C/min, the dominant crystallization reactions occur below about 400°C for all alloys under investigation. Based on this information, a temperature of 425°C was selected for the devitrification anneal. Specifically, alloy samples were encapsulated in quartz tubes under a protective atmosphere of approximately 500 mbar Argon with 99.999% purity. The encapsulated specimens were kept at 425°C for periods of 19 or 22 hrs, respectively, to ensure completion of the crystallization reaction and grain growth to a size that facilitates experimental characterization.

Figure 7 shows an X-ray diffractogram of Alloy 1A after devitrification at 425°C for 22 hours. At this point transformations I-III are fully completed and the ribbons are fully devitrified in the sense that no significant amount of amorphous material can be detected by XRD and TEM. The peak positions of (111), (200), and (220) reflections calculated for FCC pure Al (lattice parameter 4.0496 Å) are indicated in red. Within the accuracy of this experiment (that is 0.01° at $2\theta = 38.505^\circ$ (Al (111))), the measured peak positions are identical to pure Al, indicating the equilibrium solubility of Ni, Co, Yb, and Er in Al is very small. Also marked in red are the positions of the 'forbidden' reflections (110), (210), (211), and (221) for FCC Al, which are superlattice reflections of the L1₂ structure. The peak positions for L1₂ Al₃Yb (lattice parameter 4.202 Å marked in green, and that for L1₂ Al₃Er (lattice parameter 4.215 Å) are marked in brown. It can be seen that the measured peak positions are perfectly matched by L1₂ structure reflections. Therefore, Alloy 1A mainly consists of FCC Al and L1₂ phases as devitrified microstructure. It is also noticed that there is a minor third phase x, which crystalline structure is to be identified.

The FCC Al+L₁₂ microstructure of Alloy 1A was investigated by the secondary ion mass spectrometry (SIMS) technology. Figure 8 indicates that Yb and Er partition together into L₁₂ precipitates, while Ni and Co have limited partitions.

- The morphology of FCC+L₁₂ microstructure of Alloy 1A is shown in Figure 9.
- 5 This SEM secondary electron image indicates that the majority of L₁₂ precipitates are less than 1 micron after devitrification at 425°C, 22 hours. Based upon previously discussed experience in devitrified Al alloys, this indicated the potential to obtain nanoscale L₁₂ precipitates with thermomechanical processing.

- The three dimension atom probe microscopy (3DAPM) analysis confirms that
- 10 L₁₂ exists in Alloy 1A with formula Al_{0.72}(Yb,Er)_{0.28}. Yb and Er have about the same site fraction. Ni and Co are negligible in L₁₂ phase. See Figure 10.

- Alloy 1A was also studied through microhardness testing in ribbon conditions after thermal cycles required for powder consolidation and extrusion. Results are presented in Table 6. Through devitrification at a temperature near 300°C, Alloy 1A has demonstrated a
- 15 hardness of 490 VHN, which is equivalent to the room temperature tensile strength exceeding 1000 MPa according to Inoue's work in similar alloy systems. (Akihisa Inoue, "Amorphous, nanoquasicrystalline and nanocrystalline alloys in Al-based systems", Progress in Materials Science 43 (1998) 365-520). This result indicates high efficient strengthening of L₁₂.

20 Table 6 Microhardness testing of Alloy 1A

Condition	Hardness (VHN)
As-spun	369
177°C 1hr	276
177°C 10hrs	310
177°C 20 hrs	335
177°C 20hrs then 288°C 2hrs.	490
177°C 20hrs then 316°C 2hrs.	340
177°C 20hrs then 400°C 2hrs.	275

Example 2

Alloy 2A in Table 5 was fabricated into ribbons using melt spinning technology (wheel speed 55 m/s). In the as melt-spun condition, Alloy 2A was characterized by X-ray diffraction. The diffractometer trace (Cu-K α radiation) of as-spun Alloy 2A in Figure 11 shows a broad

peak characteristic of glass, and the ribbons show reasonable good ductility, also characteristic of the glassy state.

Figure 12 shows an X-ray diffractogram of Alloy 2A after devitrification at 425°C for 19 hours. At this point the ribbon is fully devitrified in the sense that no significant amount of amorphous material can be detected by XRD. The peak positions of (111), (200), and (220) reflections calculated for FCC pure Al (lattice parameter 0.40496 Å) are indicated in red. The measured peak positions are identical to pure Al, indicating the equilibrium solubility of Ni, Co, Yb, and Er in Al is very small. Also marked in red are the positions of the 'forbidden' reflections (110), (210), (211), and (221) for FCC Al, which are superlattice reflections of the L₁₂ structure. The peak positions for L₁₂ Al₃Yb (lattice parameter 4.202 Å) are marked in green, and that for L₁₂ Al₃Er (lattice parameter 4.215 Å) are marked in brown. It can be seen that the measured peak positions are perfectly matched by L₁₂ structure reflections. Therefore, Alloy 2A mainly consists of FCC Al and L₁₂ phases as devitrified microstructure. It is noticed that the third phase χ , in Example 2A, is less than in Example 1A, reflecting the desire to reduce the amount of χ phase by reducing Ni and Co in Alloy 2A while retaining reasonable glass forming ability.

Example 3

Alloy 2B in Table 5 was fabricated into ribbons using melt spinning technology (wheel speed 55 m/s). In the as melt-spun condition, Alloy 2B was characterized by X-ray diffraction. The diffractometer trace (Cu-K α radiation) of as-spun Alloy 2B in Figure 13 shows a broad peak characteristic of glass, and the ribbons show reasonable good ductility, also characteristic of the glassy state.

Figure 14 shows an X-ray diffractogram of Alloy 2B after devitrification at 425°C for 19 hours. At this point the ribbon is fully devitrified in the sense that no significant amount of amorphous material can be detected by X-ray diffraction (XRD). The peak positions of (111), (200), and (220) reflections calculated for FCC pure Al (lattice parameter 4.0496 Å) are indicated in red. The measured peak positions are identical to pure Al, indicating the equilibrium solubility of Ni, Co, Yb, Er and Sc in Al is very small. Also marked in red are the positions of the 'forbidden' reflections (110), (210), (211), and (221) for FCC Al, which are superlattice reflections of the L₁₂ structure. It can be seen that the measured peak positions are matched by L₁₂ structure reflections with lattice parameter 4.150 Å. It demonstrates that Yb, Er and Sc can be completely intersoluble to form L₁₂, and the lattice parameter has been

significantly reduced by adding Sc, which is another means of reducing misfit to keep the $L1_2$ precipitates coarsening resistant. The misfit between FCC Al and $L1_2$ is 2.52% for Alloy 2B.

Example 4

5 Alloy 2C in Table 5 was fabricated into ribbons using melt spinning technology (wheel speed 55 m/s). In the as melt-spun condition, Alloy 2C was characterized by X-ray diffraction. The diffractometer trace (Cu-K α radiation) of as-spun Alloy 2C in Figure 15 shows a broad peak characteristic of glass, and the ribbons show reasonable good ductility, also characteristic of the glassy state.

10 Figure 16 shows an X-ray diffractogram of Alloy 2C after devitrification at 425°C for 19 hours. At this point the ribbon is fully devitrified in the sense that no significant amount of amorphous material can be detected by XRD. The peak positions of (111), (200), and (220) reflections calculated for FCC pure Al (lattice parameter 4.0496 Å) are indicated in red. The measured peak positions indicate that the lattice space of Al has been dilated to 4.060 Å,
15 reflecting another feature of the invention: adding Mg to expand the lattice space of Al and thus decrease the misfit between Al and $L1_2$. Also marked in red are the positions of the 'forbidden' reflections (110), (210), (211), and (221) for FCC Al, which are superlattice reflections of the $L1_2$ structure. It can be seen that the measured peak positions are perfectly matched by $L1_2$ structure reflections. Therefore, Alloy 2C mainly consists of FCC Al and $L1_2$ phases as
20 devitrified microstructure.

Example 5

Alloy 2D in Table 5 was fabricated into ribbons using melt spinning technology (wheel speed 55 m/s). In the as melt-spun condition, Alloy 2D was characterized by X-ray diffraction.
25 The diffractometer trace (Cu-K α radiation) of as-spun Alloy 2D in Figure 17 shows a broad peak characteristic of glass, and the ribbons show very good ductility, also characteristic of the glassy state.

Figure 18 shows an X-ray diffractogram of Alloy 2D after devitrification at 425°C for 19 hours. At this point the ribbon is fully devitrified in the sense that no significant amount of
30 amorphous material can be detected by XRD. The peak positions of (111), (200), and (220) reflections calculated for FCC pure Al (lattice parameter 4.0496 Å) are indicated in red. The measured peak positions indicate that the lattice space of Al has been dilated to 4.057 Å. Also marked in red are the positions of the 'forbidden' reflections (110), (210), (211), and (221) for

FCC Al, which are superlattice reflections of the $L1_2$ structure. It can be seen that the measured peak positions are matched by $L1_2$ structure reflections with lattice parameter 4.155 Å. It demonstrates that Yb, Er and Sc can be completely intersoluble to form $L1_2$, and the lattice parameter has been significantly reduced by adding Sc. Alloy 2D reflects the means of reducing misfit by adding Mg to dilate the lattice space of Al and adding Sc to decrease the lattice parameter of $L1_2$. Thus Alloy 2D achieved the lowest misfit so far: 2.42% without losing the glass forming ability. Alloy 2D mainly consists of FCC Al and $L1_2$ phases as devitrified microstructure.

10 Example 6

Alloy 1E in Table 5 was fabricated into ribbons using melt spinning technology (wheel speed 55 m/s). In the as melt-spun condition, Alloy 1E was characterized by X-ray diffraction. The diffractometer trace (Cu-K α radiation) of as-spun Alloy 1E in Figure 19 shows crystalline reflection peaks, indicating non-amorphous or partially non-amorphous state. It demonstrates that TMs are necessary elements to promote glass in Al-TM-RE system. In addition, the ribbons are very brittle, also characteristic of the non-glassy state.

Figure 20 shows an X-ray diffractogram of Alloy 1E after devitrification at 425°C for 19 hours. This diffractogram shows that Alloy 1E only has two phases: fcc Al+ $L1_2$. It also demonstrates that Yb, Er and Sc can be completely intersoluble to form $L1_2$, and the lattice parameter has been significantly reduced by adding Sc. The misfit between FCC Al and $L1_2$ is 3.03%.

The morphology of fcc+ $L1_2$ microstructure of Alloy 1E is shown in Figure 21. This SEM secondary electron image indicates that the particle size of $L1_2$ precipitates is about 3 times larger than that of Alloy 1A, see Figure 9, although the misfit of Alloy 1A is a little bit larger: 3.735%. It indicates that devitrification of glassy state can significantly reduce the particle size of precipitation in comparison with that by crystallization directly from fast cooling at the same rate.

In review, the range of composition processing parameters, microstructure characterization and physical properties is summarized in the following Table 7:

Table 7

	Composition				Processing Parameters			microstructure characterization (vol %)								Properties	
	Rare Earth Elem.	Transition Metals and Mg, Li			glass	thermal	thermo-mechanical	amorphous				devitrified state				room temperature UTS	high temperature UTS of 275-410 MPa
	(1)	Late TM for glass forming (2)	L12 modifier (3)	FCC elem. For misfit (4)	at.%	RSP	aging temp. for thermal devitrifying	hot extrusion parameters	fcc	glass	others	fcc	L12	glass	others		
Maximum Ranges	Er, Lu, Yb, Tm, U	Ni, Co, Fe, Cu	Sc, Y, Ti, Zr, V, Cr, Mn, Li, Nb	Mg, Zn, Ag	2% < sum(group (1)) < 15% 2% < sum(group (2)) < 7% sum(group (3)) < 5% sum(group (4)) < 7%	cooling rate > 10 ⁴ °C/sec	> 300 °C		< 15%	bal.	< 10%	bal.	> 10%	< 15%	< 20%	> 500 MPa	> 250 °C
Preferred Ranges	Er, Lu, Yb, Tm	Ni, Co	Sc	Mg	5% < sum(group (1)) < 12% 2% < sum(group (2)) < 7% Sc < 4% Mg < 8%	cooling rate > 10 ⁴ °C/sec	> 325 °C < 475 °C	> 350 °C < 450 °C 5, 8, 11:1 ratio	< 8%	bal.	< 3%	bal.	> 20-25%	< 8%	< 15%	> 800 MPa	> 275 °C
Optimum Ranges	Er, Yb	Ni, Co	Sc		7% < sum(Er, Yb, Sc) < 8% 3% < sum(Ni, Co) < 8%	> 10 ⁴ °C/sec, atomized powder with -325 mesh	> 370 °C < 450 °C	400 °C 11:1 ratio	< 5%	bal.	< 1%	bal.	> 30%	< 3%	< 5%	> 1000 MPa	> 300 °C
Examples	Er, Yb	Ni, Co	Sc, Y	Mg	7% < sum(Er, Yb) < 8% sum(Ni, Co) < 5.5% sum(Sc, Y) < 5%, Mg < 3%	about 10 ⁴ °C/sec	425 °C	400 °C 11:1 ratio	100% or < 20%			bal.	> 28% < 32%	< 3%	< 15-20%	490 VHN (1A) which is > 1000 MPa	
Preferred Methods:																	
Atomization and consolidation with extrusion																	

Variations of the described aluminum alloy as well as the process for manufacture thereof and the product created by the process are available to provide the expected functionality of high short-term and long-term strength at temperatures above about 300°C. Thus the invention is to be limited only by the following claims and equivalents thereof.

CLAIMS

What is claimed is:

1. An aluminum alloy characterized by high strength including high strength in the temperature range greater than about 250°C comprising, in combination:

5 an alloy mixture in primarily crystalline form having at least about 30% by volume fcc phase and at least about 10% by volume L1₂ ductile precipitate phase, said alloy consisting essentially of at least one transition metal selected from the group consisting of about 2 to 12 atomic percent Ni, Co, Ti, Fe, Y, Sc, Cu, Zn, V, Cr, Mn and Li, and at least one rare earth material selected from the group consisting of about 2 to
10 15 atomic percent Er, Tm, Yb, Lu, and the balance Al.

2. The alloy of claim 1 further including Mg in an amount up to about 5% atomic fraction.

3. The alloy of claim 1 having a tensile strength of at least about 275Mpa at 250°C.

4. A method for manufacture of an aluminum alloy characterized by high strength including high strength in a temperature range greater than about 250°C comprising the steps
15 of:

(a) forming a melt mixture of aluminum, about 2 to about 12 atomic percent of at least one metal selected from the group consisting of Ni, Co, Ti, Fe, Y, Sc, Cu, Zn, V, Cr, Mn and Li, and at least one rare earth selected from the group consisting of about 2 to 15 atomic percent Er, Tm, Yb, and Lu;

20 (b) converting said melt to an amorphous state wherein the mixture comprises at least about 70% by volume amorphous material; and

(c) devitrifying said amorphous material to at least in part a crystalline matrix of at least about 30% by volume fcc and at least about 10% by volume L1₂ phase.

5. The method of claim 4 wherein the step of converting the melt comprises cooling in the
25 range of at least about 10³°C per second.

6. The method of claim 4 wherein the step of devitrification is selected from a group consisting of thermoprocessing, thermomechanical processing and combinations thereof. A high temperature and high strength aluminum-based alloy processed through a primarily greater than about 70% in volume amorphous state and then devitrified into greater than about 70% in
30 volume crystalline microstructure with fcc matrix and strengthening by about a ductile L1₂ precipitate phase greater than about 10% L1₂, and fcc greater than about 30% in volume.

7. The method of claim 4 wherein converting the melt comprises a step selected from the group consisting of gas powder atomization, water powder atomization, melt spinning, spray casting and combinations thereof.
8. The method of claim 4 wherein the step of devitrifying amorphous material comprises a
5 step selected from the group consisting of hot isostatic pressing, thermal aging, extrusion and combinations thereof.
9. An aluminum alloy characterized by high strength including high strength at a temperature greater than about 250°C made by a process comprising the steps of:
- 10 (a) formulating a melt comprised of Al; at least one transition metal (TM) selected from the group consisting of Ni, Co, Ti, Fe, Y, Sc, Cu, Zn, V, Cr, Mn, Li and Mg; and at least one rare earth selected from the group consisting of Er, Tm, Yb, Lu;
- (b) converting the melt to at least about 70% by volume amorphous material; and
- 15 (c) devitrifying at least in part the amorphous material to a mixture of fcc and L1₂ crystalline precipitate phase material.
10. The alloy product by the process of claim 9 wherein the transition metal is provided in an amount of about 2 to 10 atomic percent.
11. The alloy product by the process of claim 9 wherein the rare earth material is provided in an amount of about 2 to 10 atomic percent.
- 20 12. The alloy product by the process of claim 9 further including an additive of Mg to the melt.
13. The alloy product by the process of claim 9 wherein devitrifying the amorphous material comprises forming at least about 30% by volume fcc material.
14. The alloy product by the process of claim 9 wherein devitrifying the amorphous
25 material comprises forming at least 10% by volume L1₂ material.
15. The alloy product by the process of claim 9 wherein converting the melt to amorphous material comprises at least one step selected from the group consisting of gas powder atomization, water powder atomization and melt spinning.
16. The alloy product by the process of claim 9 wherein devitrification comprises at least
30 one step selected from the group consisting of hot isostatic pressing, thermal aging, and extrusion.
17. The method of claim 4 wherein converting the melt comprises the step of rapid solidification processing.

18. The product by the process of claim 9 wherein converting the melt comprises rapid solidification processing.

19. The alloy of claim 1 or claim 9 wherein the precipitate phase has a grain size diameter in the range of less than about 80 nm.

Damage Tolerant Amorphous Metal Alloys

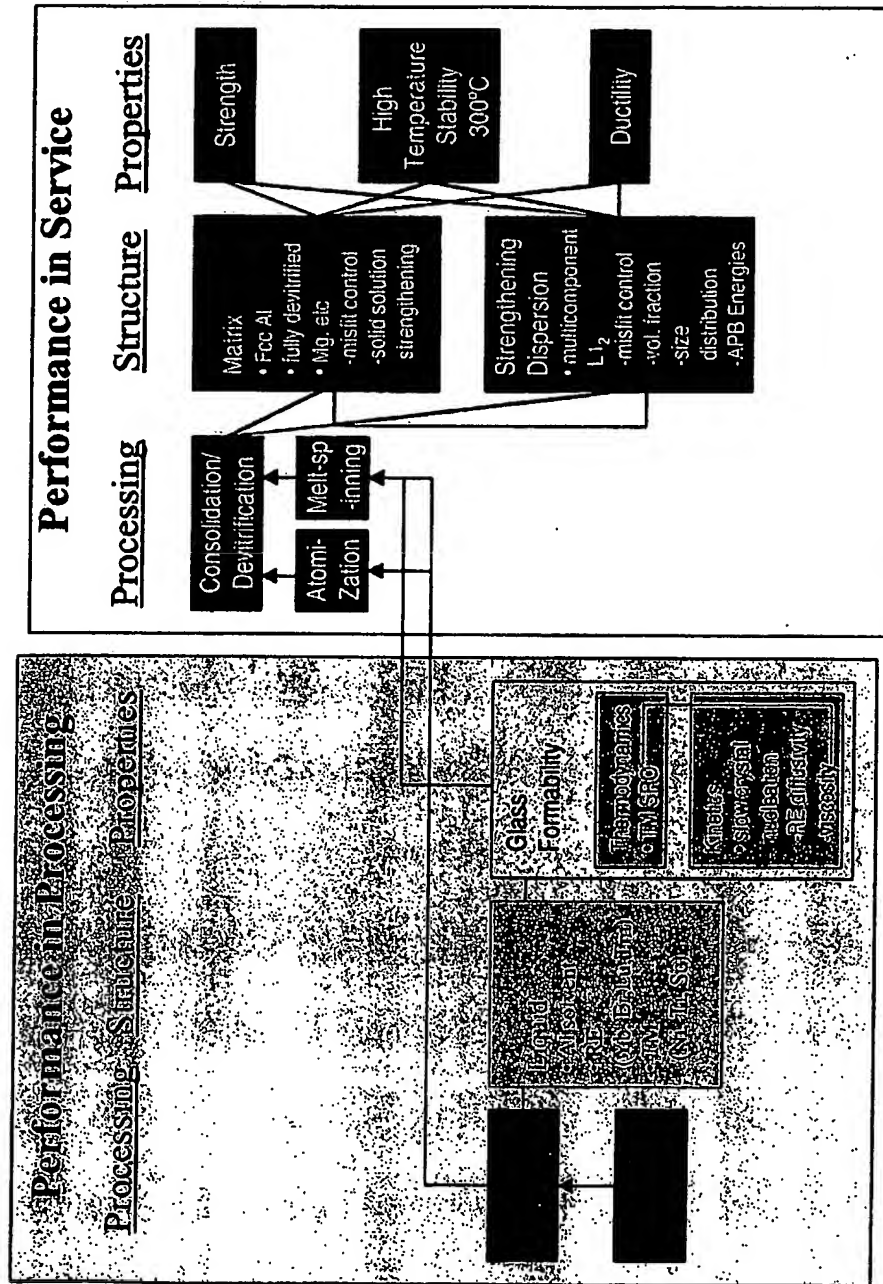


Figure 1

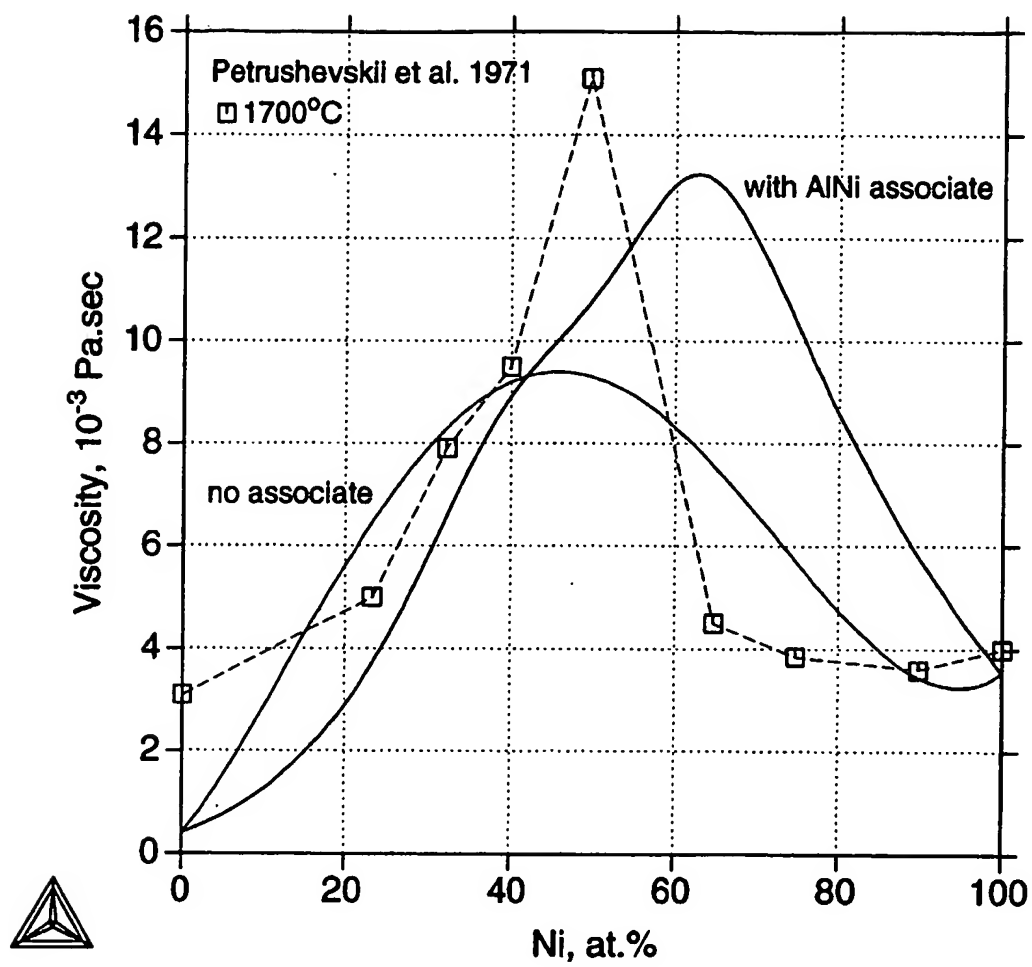


Figure 2

3/21

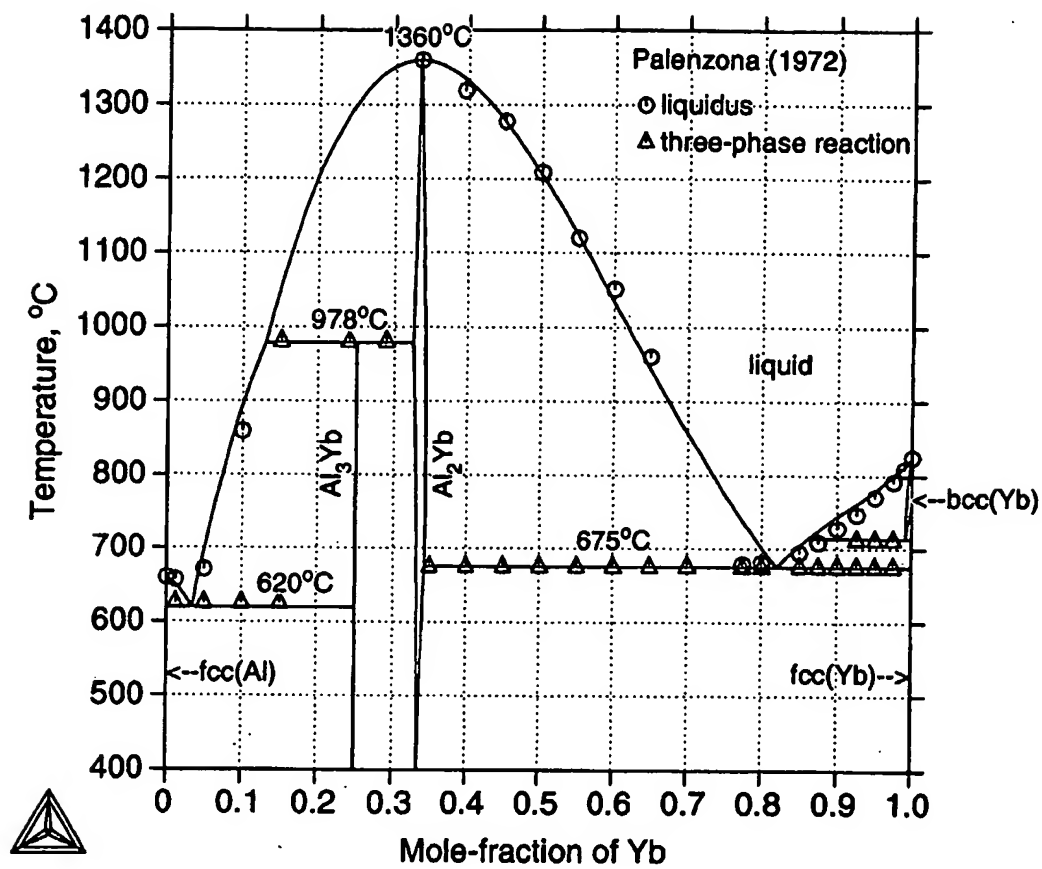


Figure 3

4/21

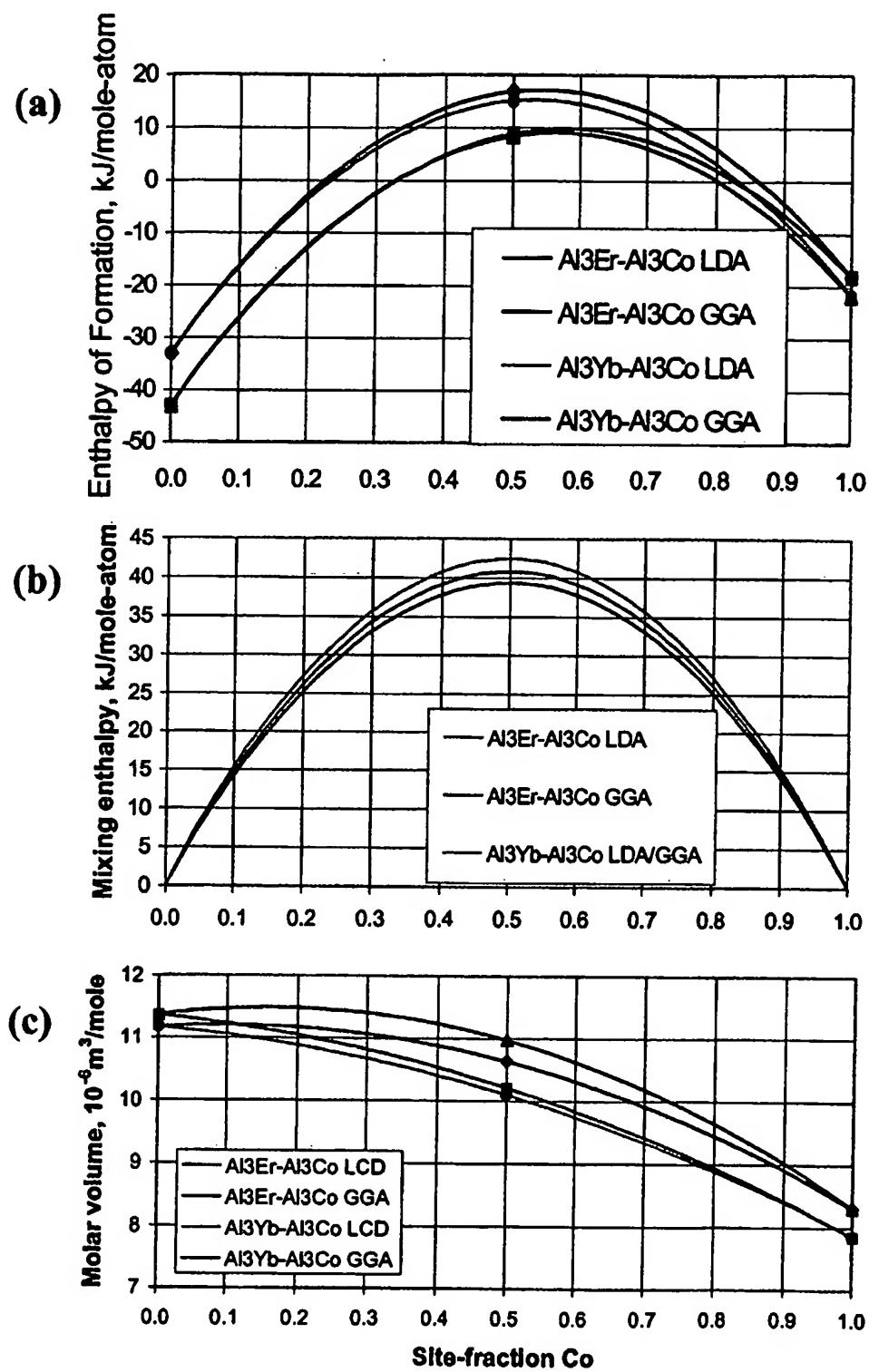


Figure 4

5/21

1A Al-Ni-Co-Yb-Er as melt-spun 55 m/s

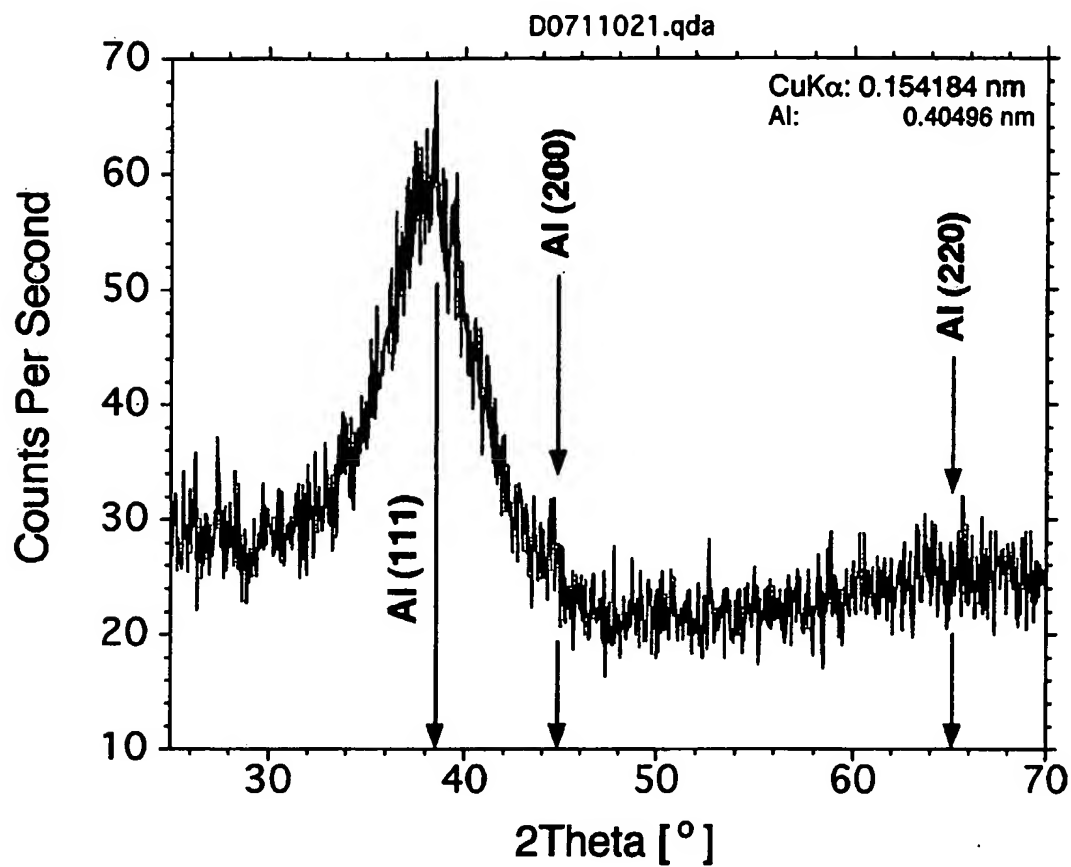


Figure 5

6/21

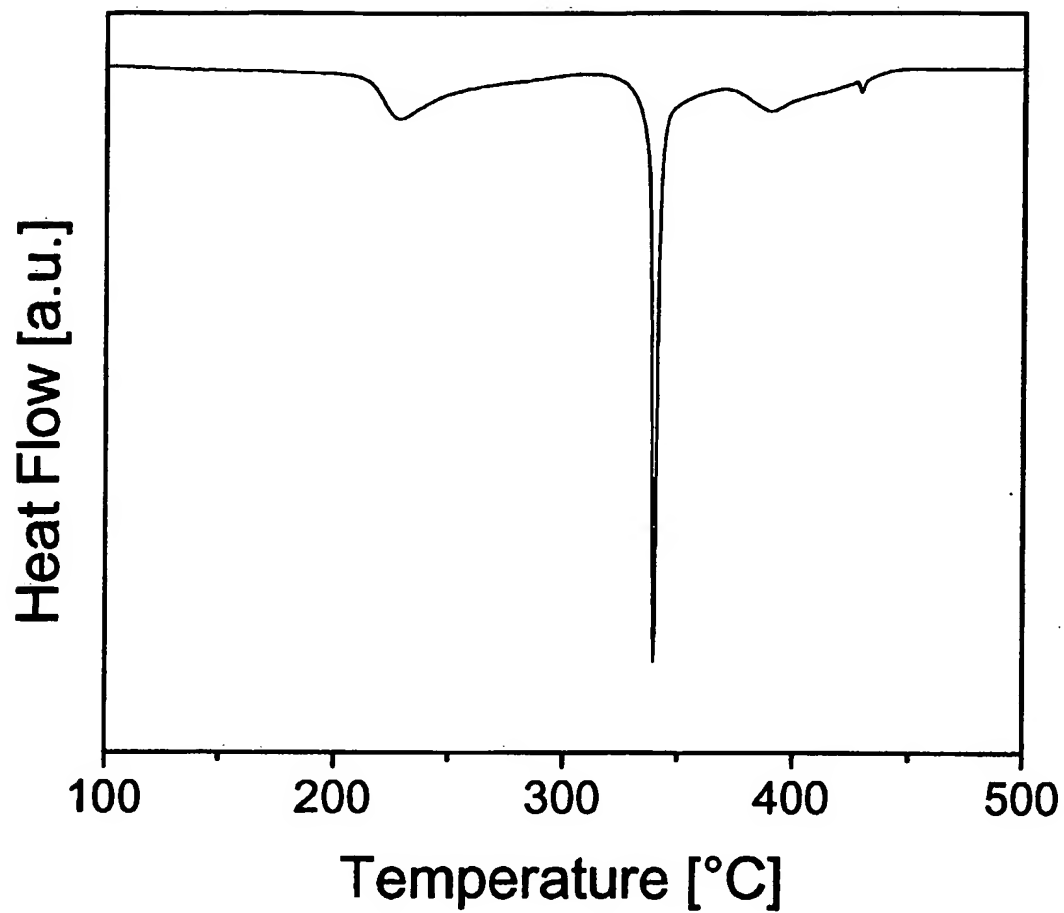


Figure 6

7/21

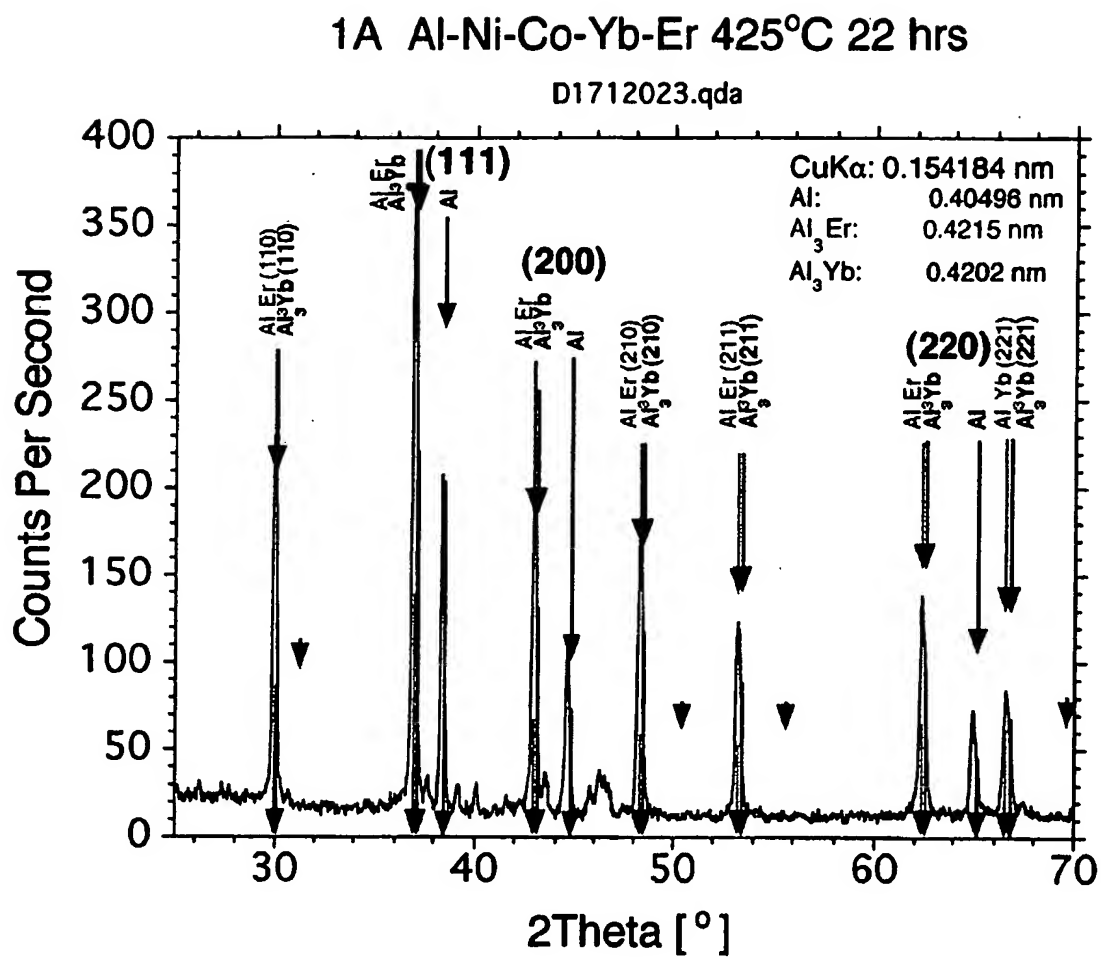
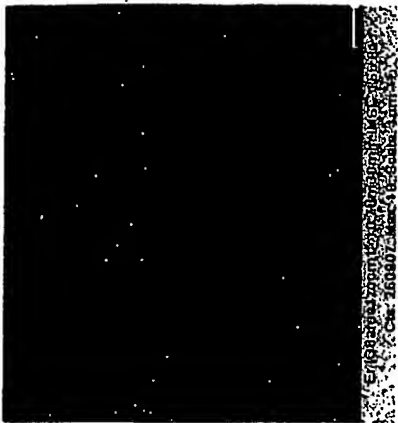
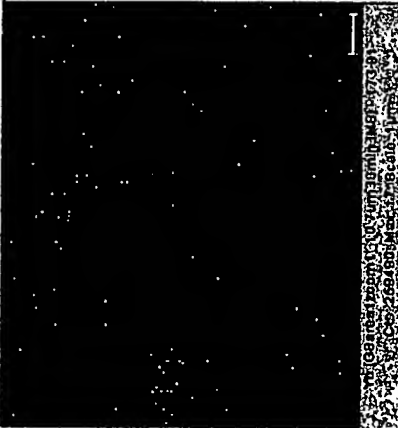


Figure 7



Er and Yb partition together to L1 phase, micron scale



Line scan shows limited Ni Co partitioning

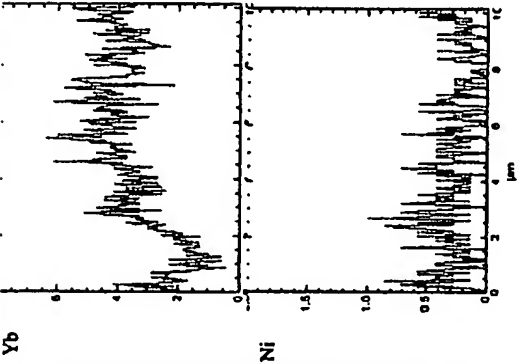
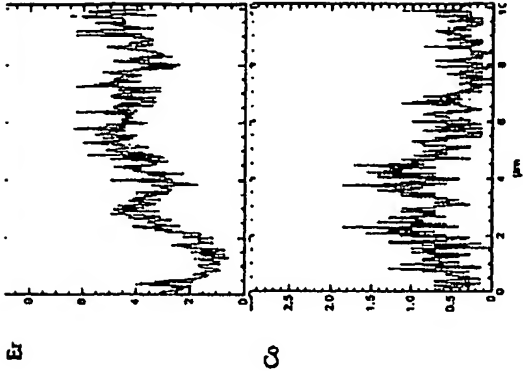
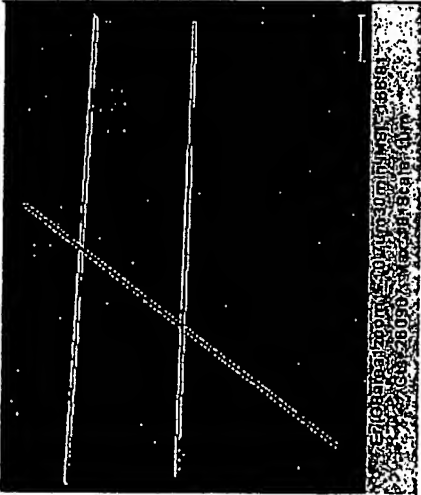


Figure 8

9/21

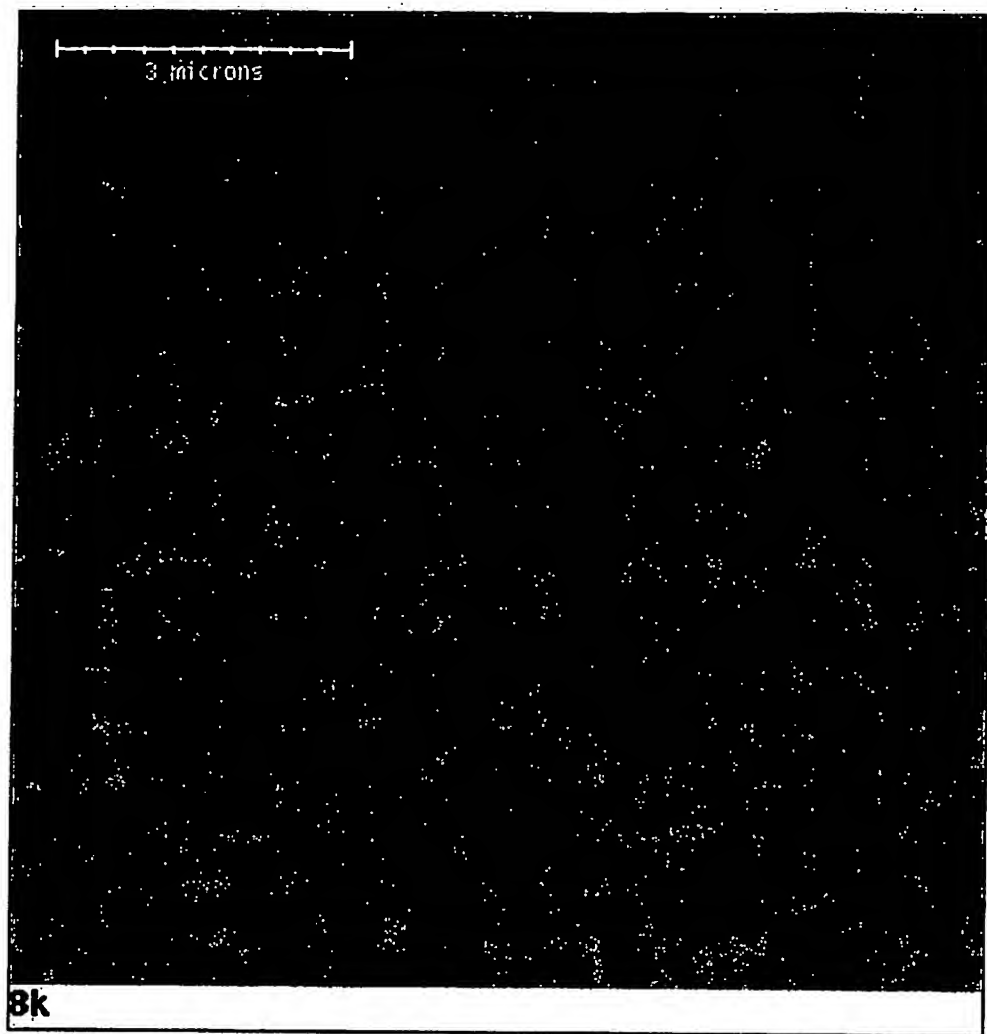


Figure 9

10/21

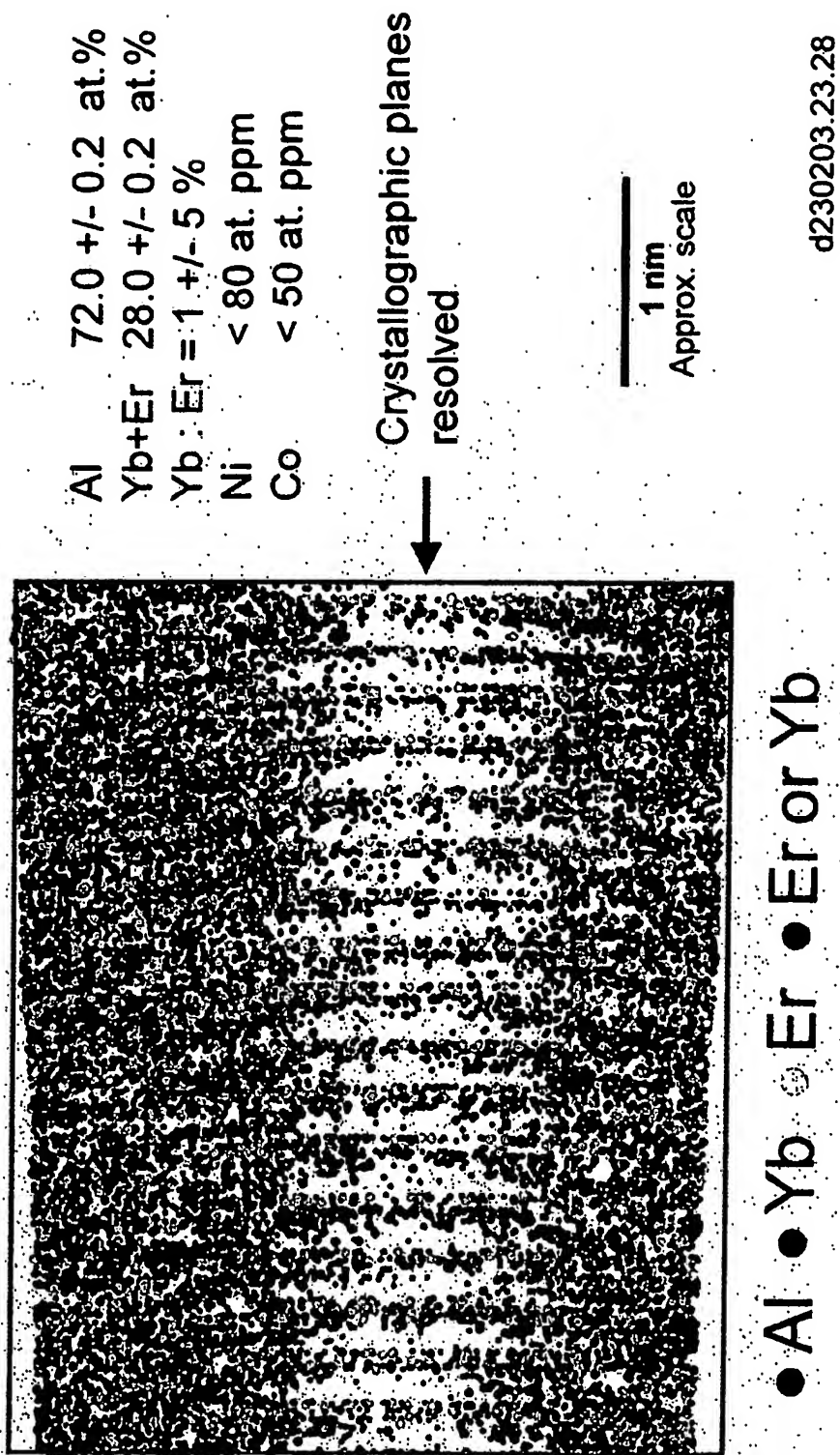


Figure 10

11/21

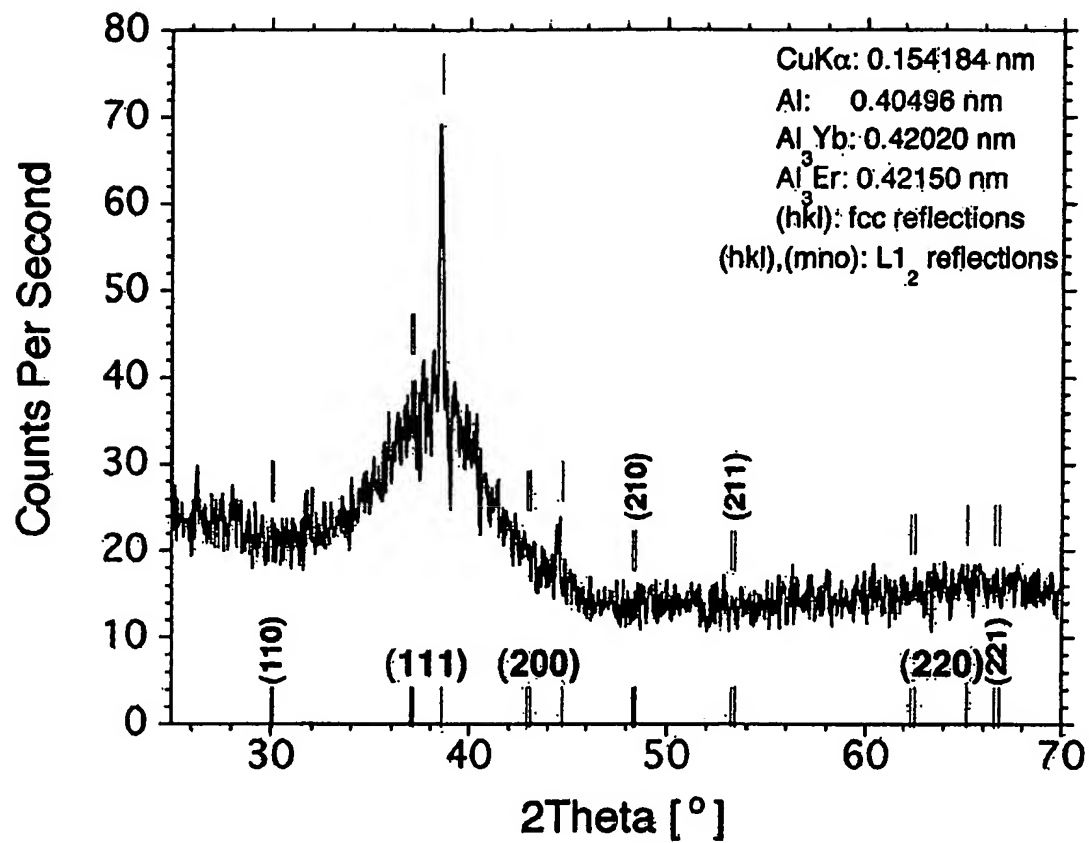


Figure 11

12/21

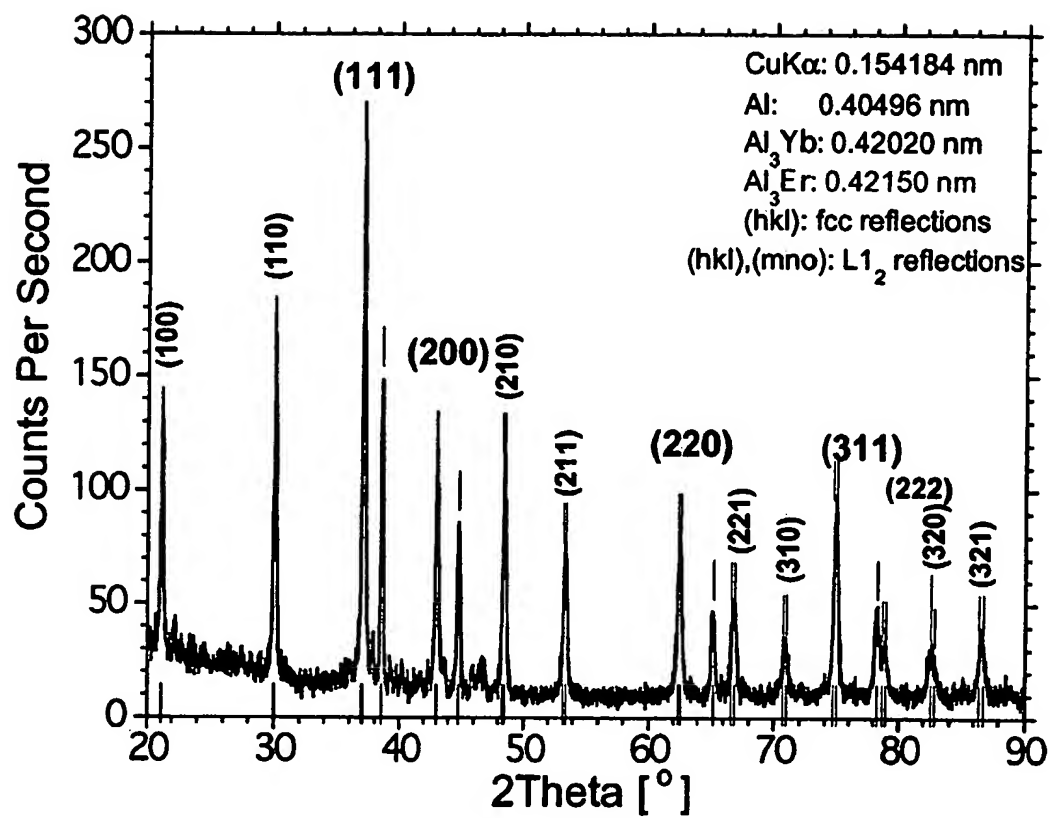


Figure 12

13/21

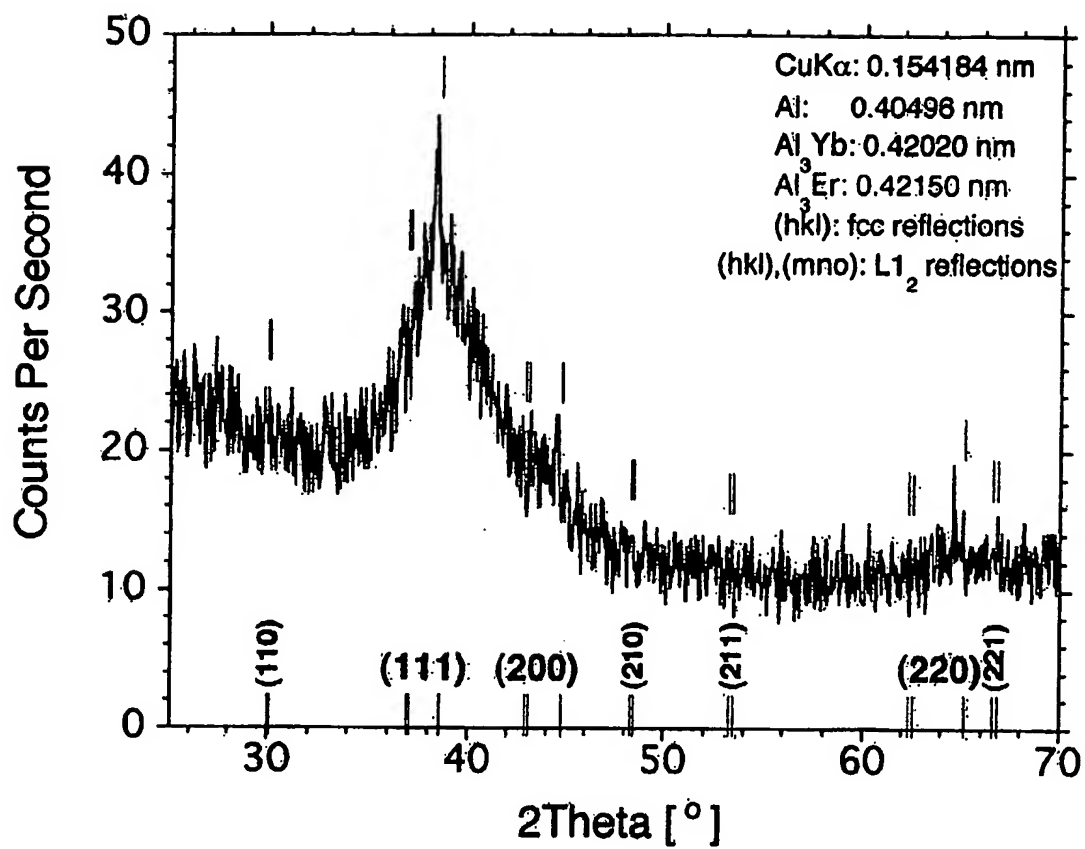


Figure 13

14/21

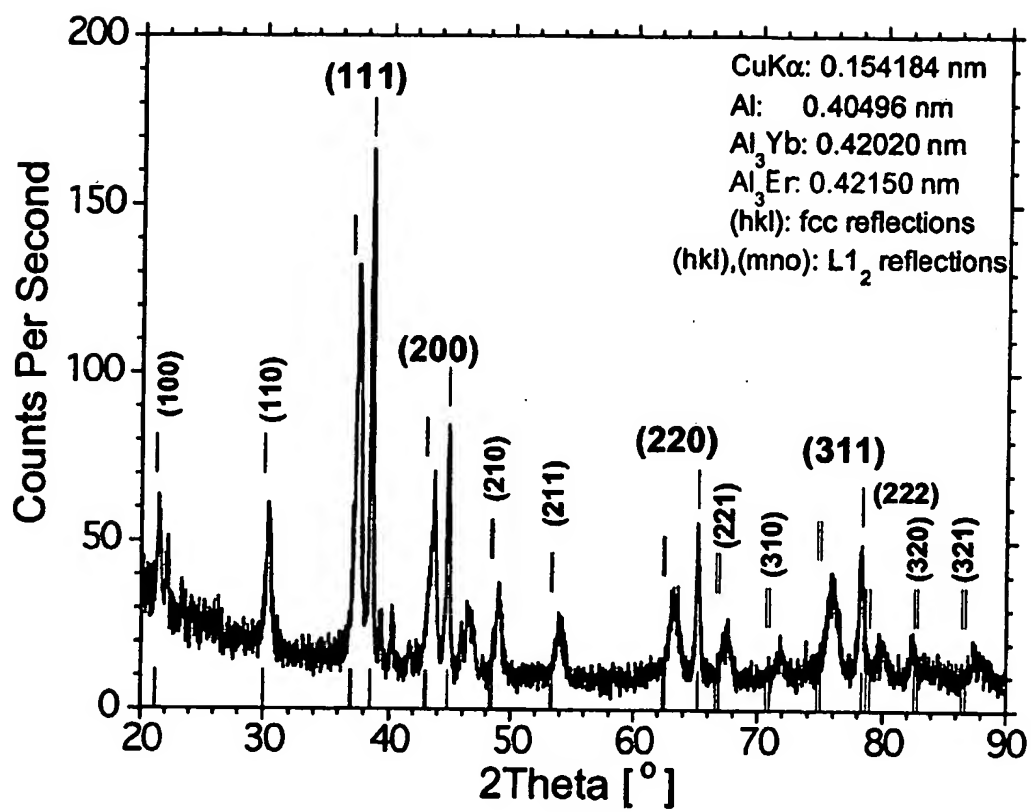


Figure 14

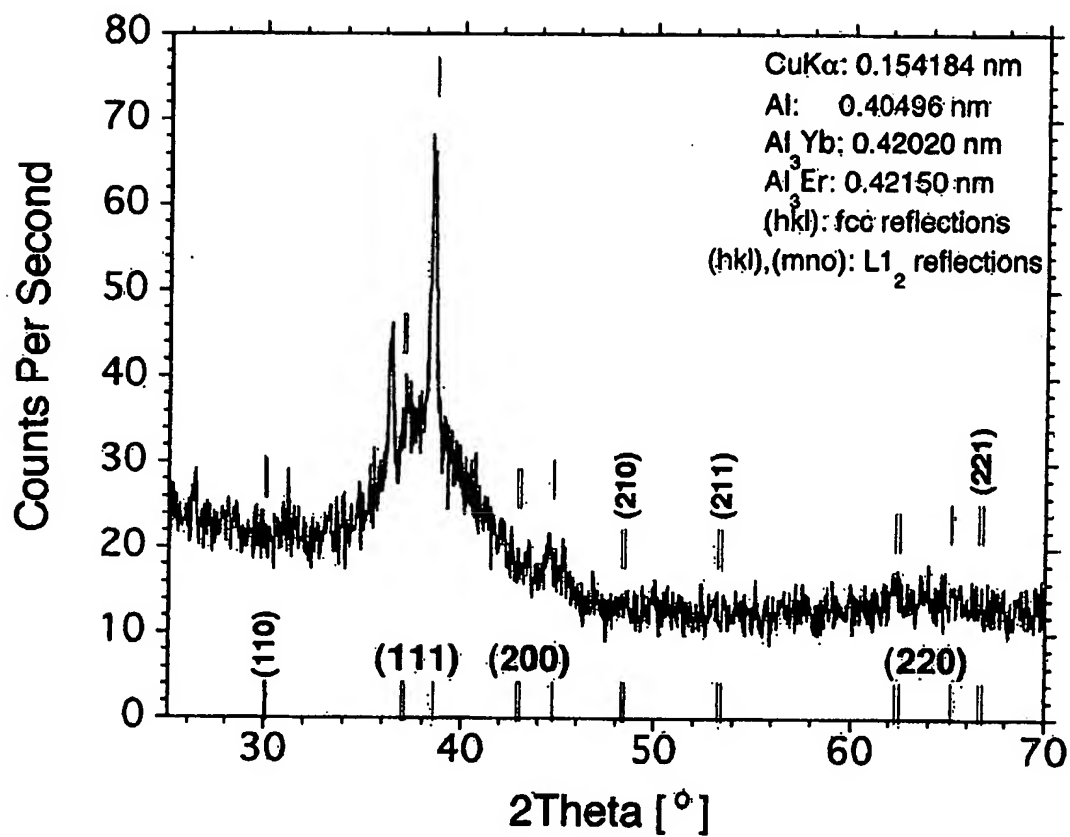


Figure 15

16/21

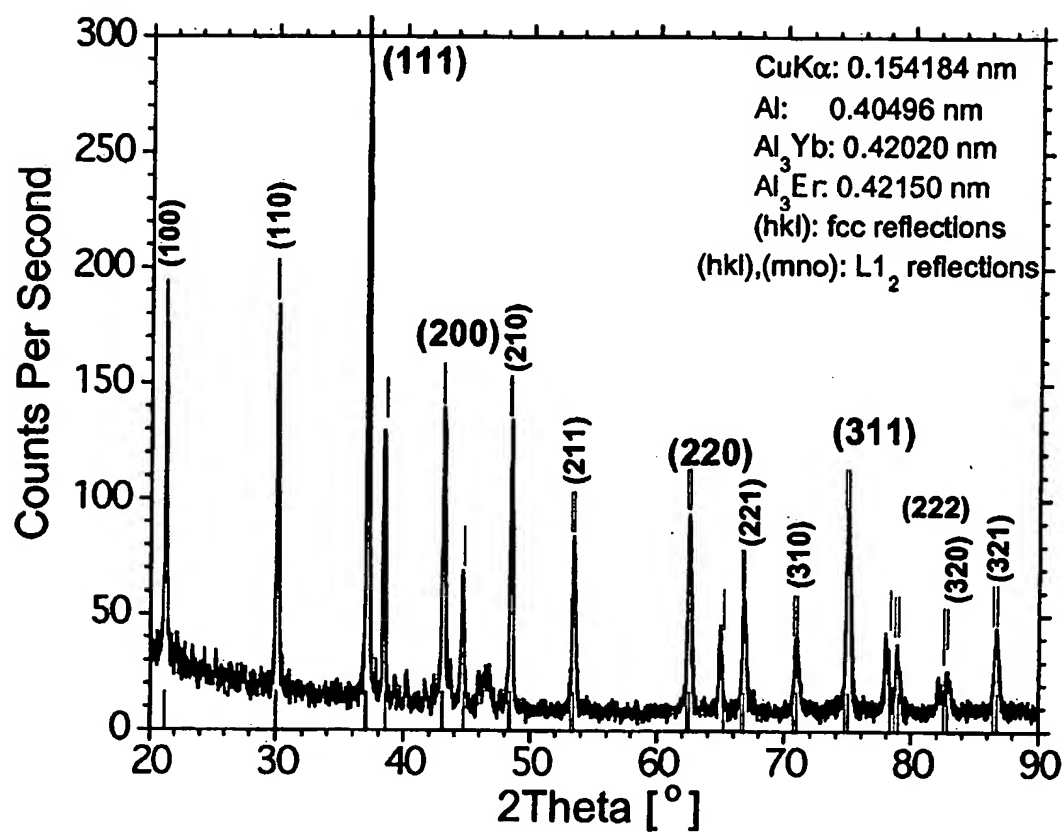


Figure 16

17/21

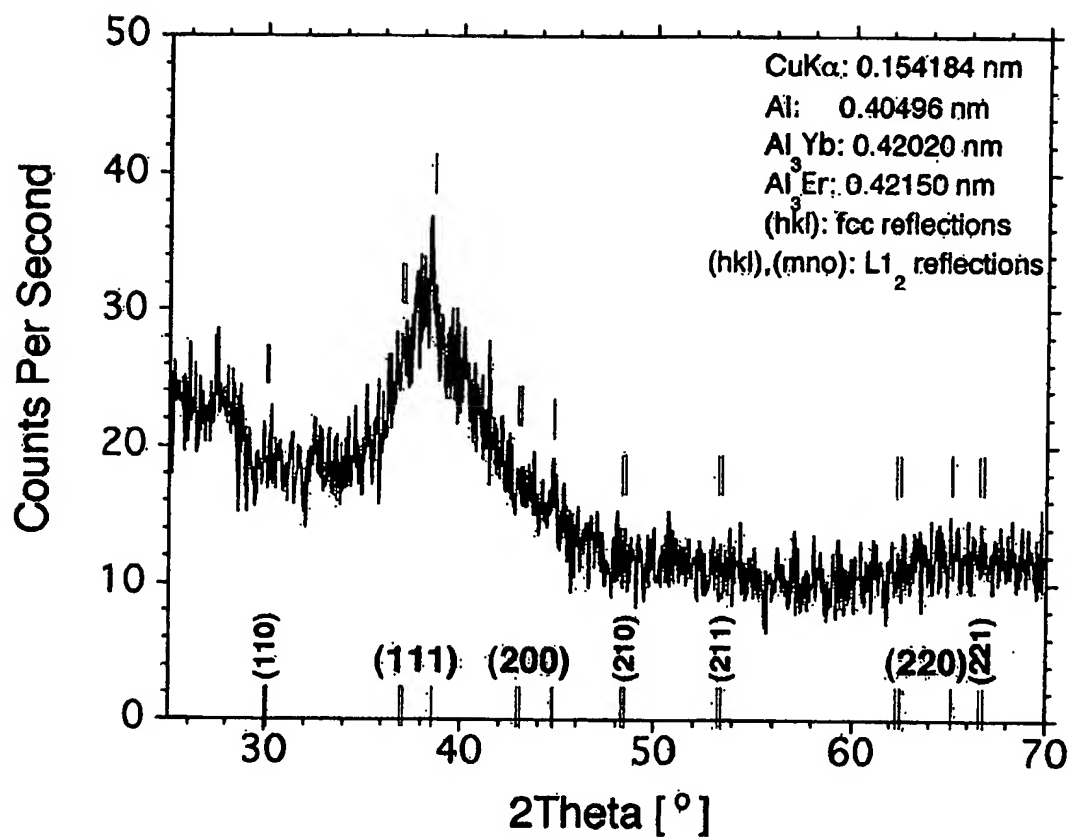


Figure 17

18/21

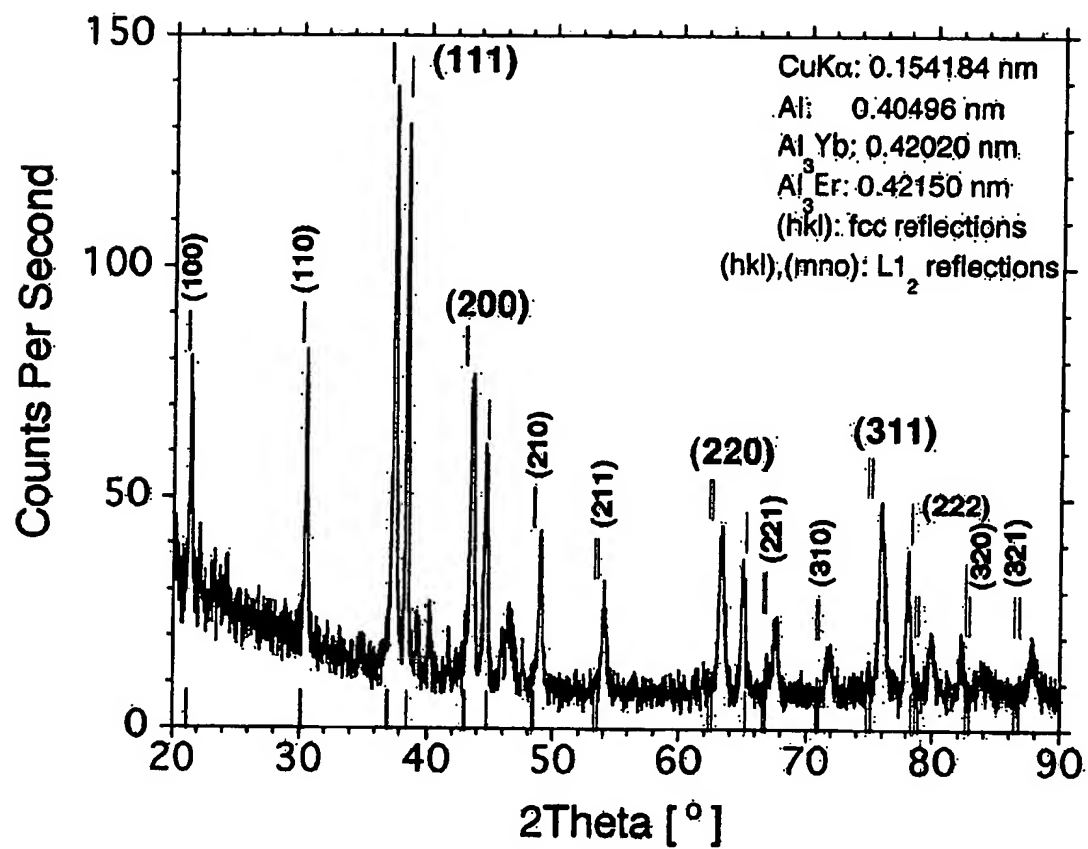


Figure 18

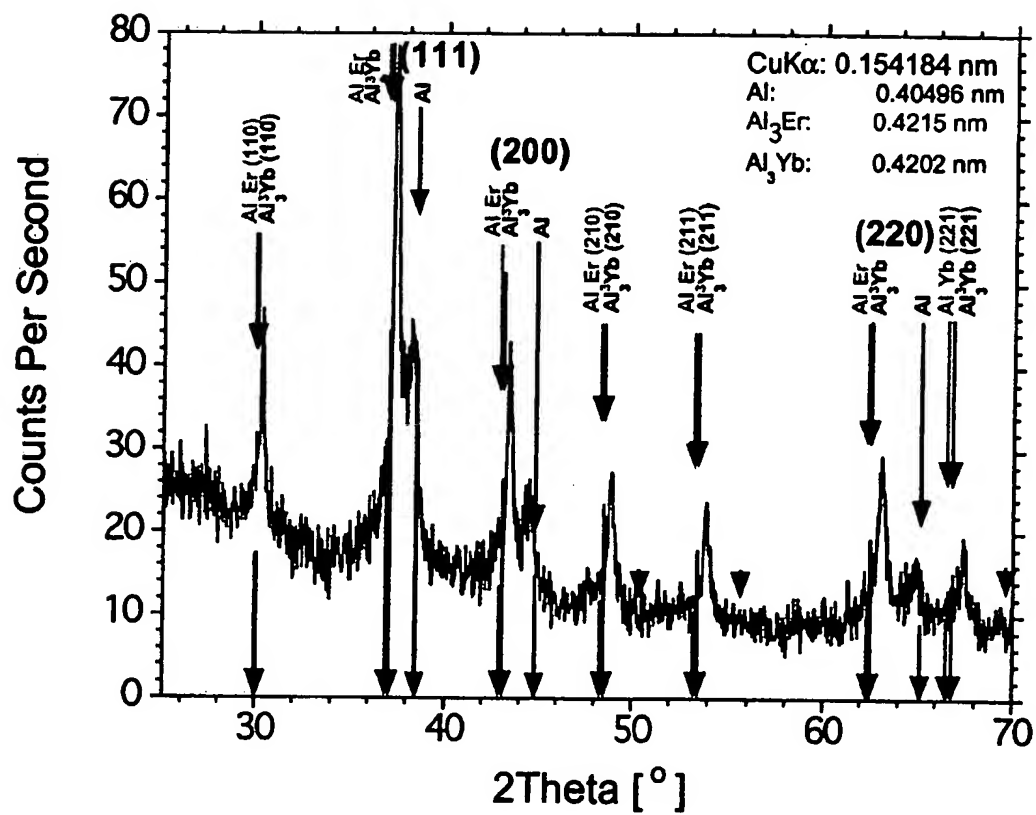


Figure 19

20/21

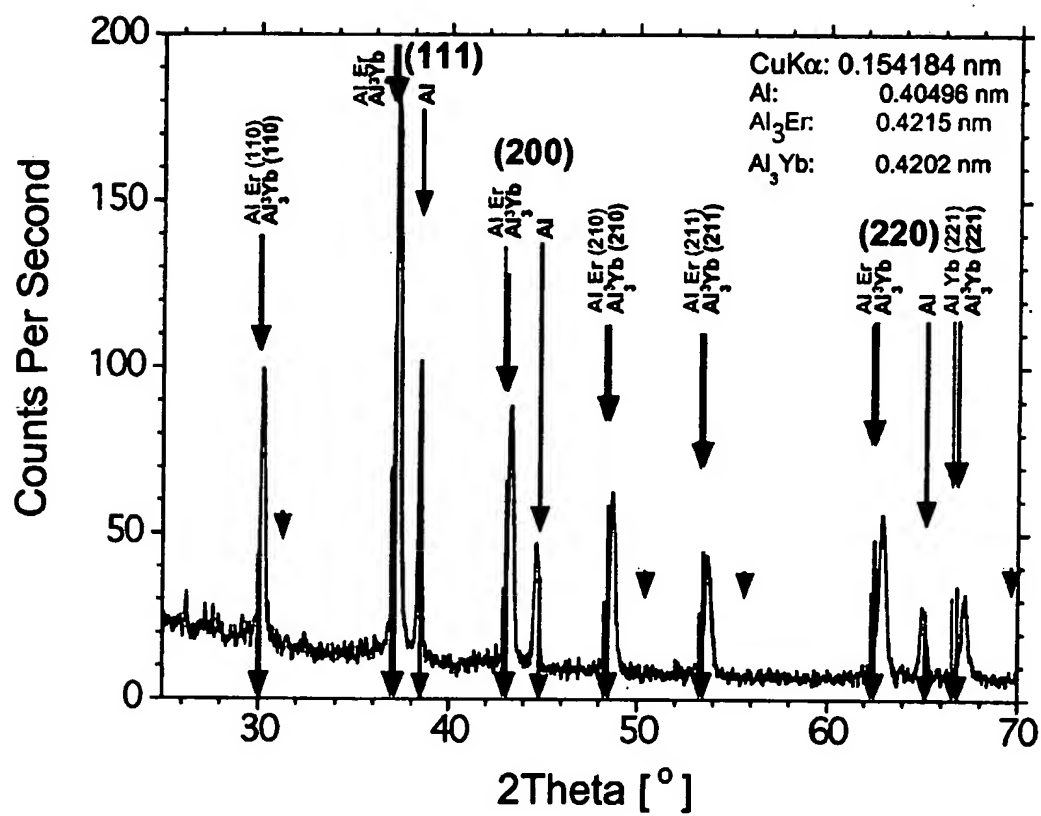


Figure 20

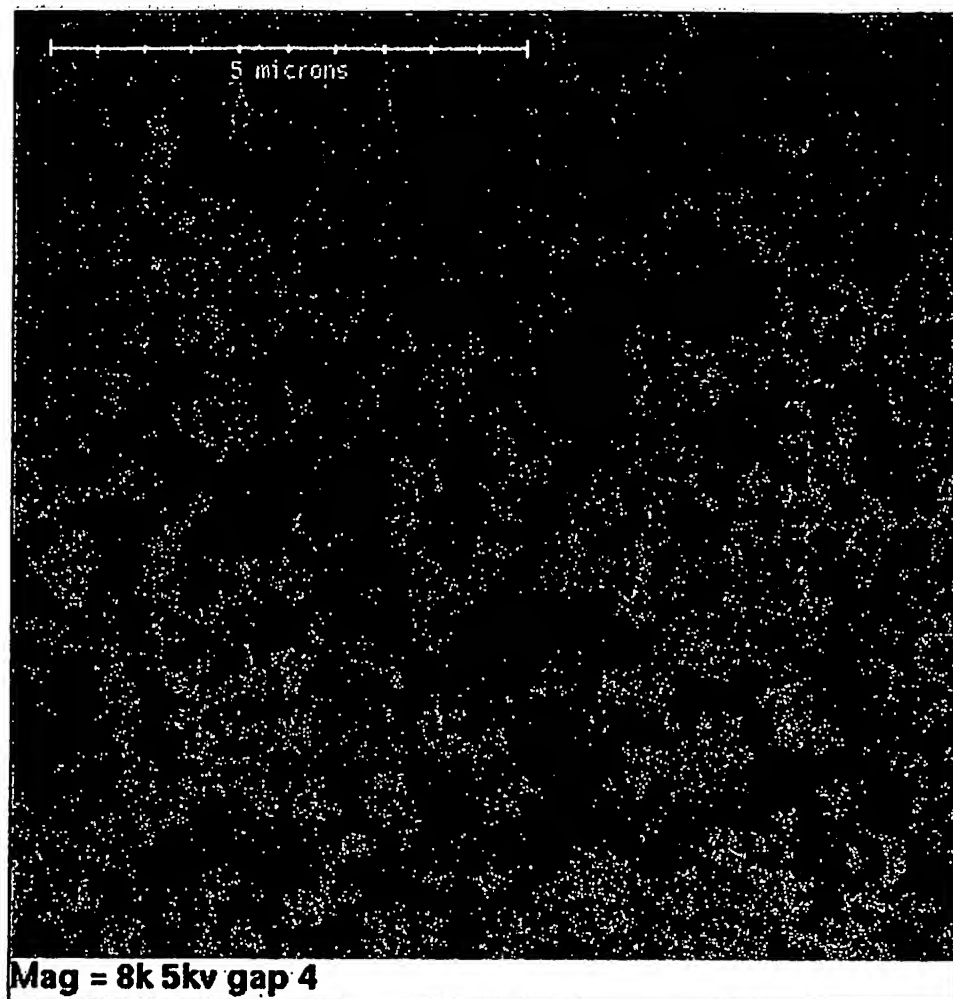


Figure 21

(19) World Intellectual Property
Organization
International Bureau



(43) International Publication Date
18 December 2003 (18.12.2003)

PCT

(10) International Publication Number
WO 2003/104505 A3

(51) International Patent Classification⁷: **C22C 45/08**,
21/00, C22F 1/04

(21) International Application Number:
PCT/US2003/012622

(22) International Filing Date: 24 April 2003 (24.04.2003)

(25) Filing Language: English

(26) Publication Language: English

(30) Priority Data:
60/375,940 24 April 2002 (24.04.2002) US
60/450,114 25 February 2003 (25.02.2003) US

(71) Applicant (for all designated States except US):
QUESTEK INNOVATIONS LLC [US/US]; 1820
Ridge Avenue, Evanston, IL 60201 (US).

(72) Inventors; and

(75) Inventors/Applicants (for US only): **OLSON, Gregory,**

B. [US/US]; 1363 Kenilwood, Riverwoods, IL 60015 (US).
TANG, Weijia [CN/US]; 3144 Greenleaf Avenue, Wil-
mette, IL 60091 (US). **QIU, Calan** [CN/US]; 3144 Green-
leaf Avenue, Wilmette, IL 60091 (US). **JOU, Herng-Jeng**
[US/US]; 1210 Manor Drive, Wilmette, IL 60091 (US).

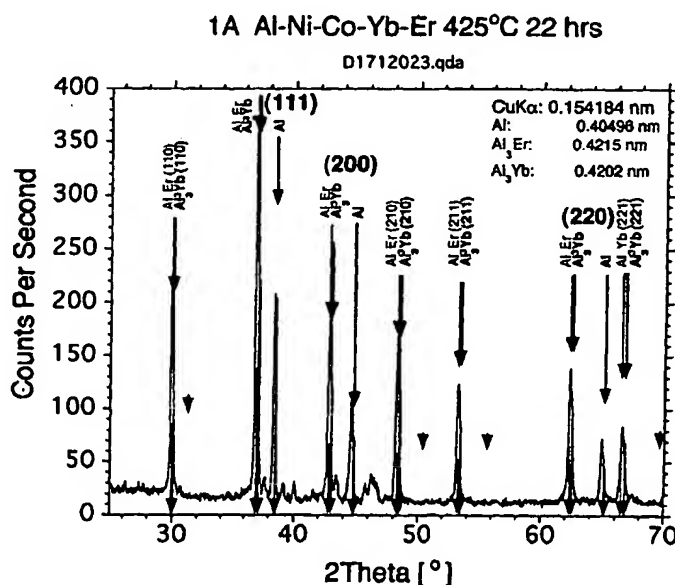
(74) Agent: **NELSON, Jon, O.**; Banner & Witcoff, Ltd., 10
South Wacker Drive, Suite 3000, Chicago, IL 60606-7402
(US).

(81) Designated States (national): AE, AG, AL, AM, AT, AU,
AZ, BA, BB, BG, BR, BY, BZ, CA, CH, CN, CO, CR, CU,
CZ, DE, DK, DM, DZ, EC, EE, ES, FI, GB, GD, GE, GH,
GM, HR, HU, ID, IL, IN, IS, JP, KE, KG, KP, KR, KZ, LC,
LK, LR, LS, LT, LU, LV, MA, MD, MG, MK, MN, MW,
MX, MZ, NI, NO, NZ, OM, PH, PL, PT, RO, RU, SC, SD,
SE, SG, SK, SL, TJ, TM, TN, TR, TT, TZ, UA, UG, US,
UZ, VC, VN, YU, ZA, ZM, ZW.

(84) Designated States (regional): ARIPO patent (GH, GM,
KE, LS, MW, MZ, SD, SL, SZ, TZ, UG, ZM, ZW),
Eurasian patent (AM, AZ, BY, KG, KZ, MD, RU, TJ, TM),
European patent (AT, BE, BG, CH, CY, CZ, DE, DK, EE,
ES, FI, FR, GB, GR, HU, IE, IT, LU, MC, NL, PT, RO,

[Continued on next page]

(54) Title: **NANOPHASE PRECIPITATION STRENGTHENED AL ALLOYS PROCESSED THROUGH THE AMORPHOUS STATE**



(57) Abstract: Aluminum alloys having improved strength characteristics at elevated temperatures (300°C) are manufactured by combining selected transition metals (Ni, Co, Ti, Fe, Y, Sc) and selected rare earth materials (Er, Tm, Yb, Lu) in amounts of about 2 to 12% and 2 to 15% atomic percent respectively in an amorphous, glassy state and subsequently devitrifying the amorphous material to form a crystalline mix of fcc and L12 phase material. Devitrification from the amorphous state may be effected by various means including thermal and thermo mechanical processes.



SE, SI, SK, TR), OAPI patent (BF, BJ, CF, CG, CI, CM, GA, GN, GQ, GW, ML, MR, NE, SN, TD, TG).

For two-letter codes and other abbreviations, refer to the "Guidance Notes on Codes and Abbreviations" appearing at the beginning of each regular issue of the PCT Gazette.

Published:

- *with international search report*
- *before the expiration of the time limit for amending the claims and to be republished in the event of receipt of amendments*

(88) Date of publication of the international search report:

18 March 2004

INTERNATIONAL SEARCH REPORT

International Application No
PCT/US 03/12622

A. CLASSIFICATION OF SUBJECT MATTER
IPC 7 C22C45/08 C22C21/00 C22F1/04

According to International Patent Classification (IPC) or to both national classification and IPC

B. FIELDS SEARCHED

Minimum documentation searched (classification system followed by classification symbols)
IPC 7 C22C C22F

Documentation searched other than minimum documentation to the extent that such documents are included in the fields searched

Electronic data base consulted during the International search (name of data base and, where practical, search terms used)

EPO-Internal, CHEM ABS Data

C. DOCUMENTS CONSIDERED TO BE RELEVANT

Category *	Citation of document, with indication, where appropriate, of the relevant passages	Relevant to claim No.
X	ABROSIMOVA G E ET AL: "PHASE TRANSFORMATIONS UPON CRYSTALLIZATION OF AMORPHOUS AL-NI-RE ALLOYS" THE PHYSICS OF METALS AND METALLOGRAPHY / FIZIKA METALLOV I METALLOVEDENIE, INTERPERIODICA PUBLISHING, XX, vol. 94, no. 1, 2002, pages 102-107, XP008025999 ISSN: 0031-918X page 102, column 2 -page 104, column 1, paragraph 1 -- -/-	1-19

☒ Further documents are listed in the continuation of box C.

☒ Patent family members are listed in annex.

* Special categories of cited documents:

"A" document defining the general state of the art which is not considered to be of particular relevance

"E" earlier document but published on or after the international filing date

"L" document which may throw doubts on priority claim(s) or which is cited to establish the publication date of another citation or other special reason (as specified)

"O" document referring to an oral disclosure, use, exhibition or other means

"P" document published prior to the international filing date but later than the priority date claimed

"T" later document published after the international filing date or priority date and not in conflict with the application but cited to understand the principle or theory underlying the invention

"X" document of particular relevance; the claimed invention cannot be considered novel or cannot be considered to involve an inventive step when the document is taken alone

"Y" document of particular relevance; the claimed invention cannot be considered to involve an inventive step when the document is combined with one or more other such documents, such combination being obvious to a person skilled in the art.

"&" document member of the same patent family

Date of the actual completion of the international search

4 February 2004

Date of mailing of the international search report

10/02/2004

Name and mailing address of the ISA

European Patent Office, P.B. 5818 Patentlaan 2
NL - 2280 HV Rijswijk
Tel. (+31-70) 340-2040, Tx. 31 651 epo nl,
Fax: (+31-70) 340-3016

Authorized officer

Gregg, N

INTERNATIONAL SEARCH REPORT

International Application No

PCT/US 03/12622

C.(Continuation) DOCUMENTS CONSIDERED TO BE RELEVANT

Category *	Citation of document, with indication, where appropriate, of the relevant passages	Relevant to claim No.
X	ARONIN A S ET AL: "FORMATION AND STRUCTURE OF NANOCRYSTALS IN AN AL86NI11YB3 ALLOY" PHYSICS OF THE SOLID STATE, AMERICAN INSTITUTE OF PHYSICS, WOODBURY, NY, US, vol. 43, no. 11, 2001, pages 2003-2011, XP001172942 ISSN: 1063-7834 page 2003, line 1 -page 2005, column 1; figure 1	1-19
X	GANGOPADHYAY A K ET AL: "EFFECT OF RARE-EARTH ATOMIC RADIUS ON THE DEVITRIFICATION OF AL88RE8NI4 AMORPHOUS ALLOYS" PHILOSOPHICAL MAGAZINE A. PHYSICS ON CONDENSED MATTER. DEFECTS AND MECHANICAL PROPERTIES, TAYLOR AND FRANCIS, LONDON, GB, vol. 80, no. 5, 2000, pages 1193-1206, XP008025988 ISSN: 0141-8610 page 1195, paragraph 3	1
A	S.WENHUI ET AL: "The Formation of Quasicrystal in Al0.77-Mn0.19-Yb0.04 by Quenching under High Static Pressure" 1991, PROC. CONF XIII AIRAPT XP008025998 page 181 -page 183	1
A	US 5 397 403 A (HORIMURA HIROYUKI ET AL) 14 March 1995 (1995-03-14)	

INTERNATIONAL SEARCH REPORT

Information on patent family members

International Application No

PCT/US 03/12622

Patent document cited in search report	Publication date	Patent family member(s)	Publication date
US 5397403 A	14-03-1995	JP 2724762 B2	09-03-1998
		JP 3202447 A	04-09-1991
		DE 4041918 A1	11-07-1991
		FR 2656629 A1	05-07-1991
		GB 2239874 A ,B	17-07-1991
		GB 2272451 A ,B	18-05-1994